Neuron
Article

Vesicular Glutamate Transporters Use Flexible Anion and Cation Binding Sites for Efficient Accumulation of Neurotransmitter

Julia Preobraschenski,[1] Johannes-Friedrich Zander,[2] Toshiharu Suzuki,[3,4] Gudrun Ahnert-Hilger,[2] and Reinhard Jahn[1,*]
[1]Department of Neurobiology, Max-Planck-Institute for Biophysical Chemistry, 37077 Göttingen, Germany
[2]AG Functional Cell Biology, Institute for Integrative Neuroanatomy, Charité University Medicine Berlin, Germany
[3]Faculty of Science and Engineering, Waseda University, Shinjuku-ku, Tokyo 169-8555, Japan
[4]Chemical Resources Laboratory, Tokyo Institute of Technology, Nagatsuta 4259, Yokohama 226-8503, Japan
*Correspondence: rjahn@gwdg.de
http://dx.doi.org/10.1016/j.neuron.2014.11.008

SUMMARY

Vesicular glutamate transporters (VGLUTs) accumulate the neurotransmitter glutamate in synaptic vesicles. Transport depends on a V-ATPase-dependent electrochemical proton gradient ($\Delta\mu H^+$) and requires chloride ions, but how chloride acts and how ionic and charge balance is maintained during transport is controversial. Using a reconstitution approach, we used an exogenous proton pump to drive VGLUT-mediated transport either in liposomes containing purified VGLUT1 or in synaptic vesicles fused with proton-pump-containing liposomes. Our data show that chloride stimulation can be induced at both sides of the membrane. Moreover, chloride competes with glutamate at high concentrations. In addition, VGLUT1 possesses a cation binding site capable of binding H^+ or K^+ ions, allowing for proton antiport or K^+/H^+ exchange. We conclude that VGLUTs contain two anion binding sites and one cation binding site, allowing the transporter to adjust to the changing ionic conditions during vesicle filling without being dependent on other transporters or channels.

INTRODUCTION

Synaptic vesicles (SVs) store neurotransmitters in presynaptic nerve endings and release them by Ca^{2+}-dependent exocytosis. SVs are then retrieved by endocytosis and locally regenerated within the nerve terminal. Before re-use, they are loaded with the respective neurotransmitters from cytoplasmic pools by means of specific vesicular neurotransmitter transporters. So far, specific transporters are known for glutamate (VGLUTs, three isoforms), glutamate and aspartate (VEAT), GABA and glycine (VGAT, also referred to as VIAAT), acetylcholine (VAChT), ATP (VNUT), and monoamines (VMATs, two isoforms). Together with the biosynthetic enzymes and the corresponding transporters in the presynaptic plasma membrane, these vesicular transporters define the neurotransmitter phenotype of a given neuron (Ahnert-Hilger et al., 2003; Edwards, 2007).

All vesicular neurotransmitter transporters are secondary active transporters that use a proton electrochemical gradient generated by a V-ATPase in the SV membrane. The V-ATPase is an electrogenic proton pump that is structurally and functionally related to the mitochondrial F_oF_1-ATPase but is unable to synthesize ATP. During each cycle a proton is translocated into the vesicle lumen, resulting in the generation of an inside positive membrane potential ($\Delta\psi$) and an outwardly directed pH gradient (ΔpH) (Muench et al., 2011; Toei et al., 2010).

Despite recent progress, we still have only an incomplete understanding of the net solute and charge movements associated with neurotransmitter (re)filling of synaptic vesicles, for several reasons. First, solutes that are either negatively charged (glutamate, aspartate), carry no net charges (GABA, glycine), or are positively charged (acetylcholine, amines) are coupled to the same electrochemical proton gradient and therefore require different transport mechanisms. Second, charge neutrality must be strictly maintained during each transport cycle. Due to the small volume of synaptic vesicles, a charge imbalance of only a single charge will already result in a membrane potential of 2 mV. The same applies to the proton balance, where (unless buffered) a single free proton in the lumen of a SV will result in a pH of 4, i.e., lower than that thought to be reached under physiological conditions (Füldner and Stadler, 1982; Nguyen and Parsons, 1995). Since a fully loaded SV contains several thousand neurotransmitter molecules, this means that after exhaustion of the vesicular buffering capacity, protons must exit SVs during transport of each neurotransmitter molecule. Indeed, VMATs, VAChT, and VGAT are coupled to the exchange of two (VMATs) or one (VGAT) protons (Hell et al., 1990; Johnson, 1988; Nguyen et al., 1998), whereas it is still unclear whether the VGLUTs operate as a proton exchanger, at least under conditions of high ΔpH (Wolosker et al., 1996), or as electrogenic uniporters (Omote and Moriyama, 2013). In the latter case, an independent exit pathway must exist for protons. Two additional proton exchangers are thought to be present in SVs that may contribute to charge and proton balance: a chloride-proton exchanger (probably ClC3) (Jentsch et al., 1999; Stobrawa et al., 2001) and a cation-proton exchanger (Goh et al., 2011). However, the evidence for the presence of these exchangers is still somewhat circumstantial and requires further corroboration.

Chloride ions play a fundamental role in vesicular neurotransmitter uptake, but it has been surprisingly difficult to unravel the

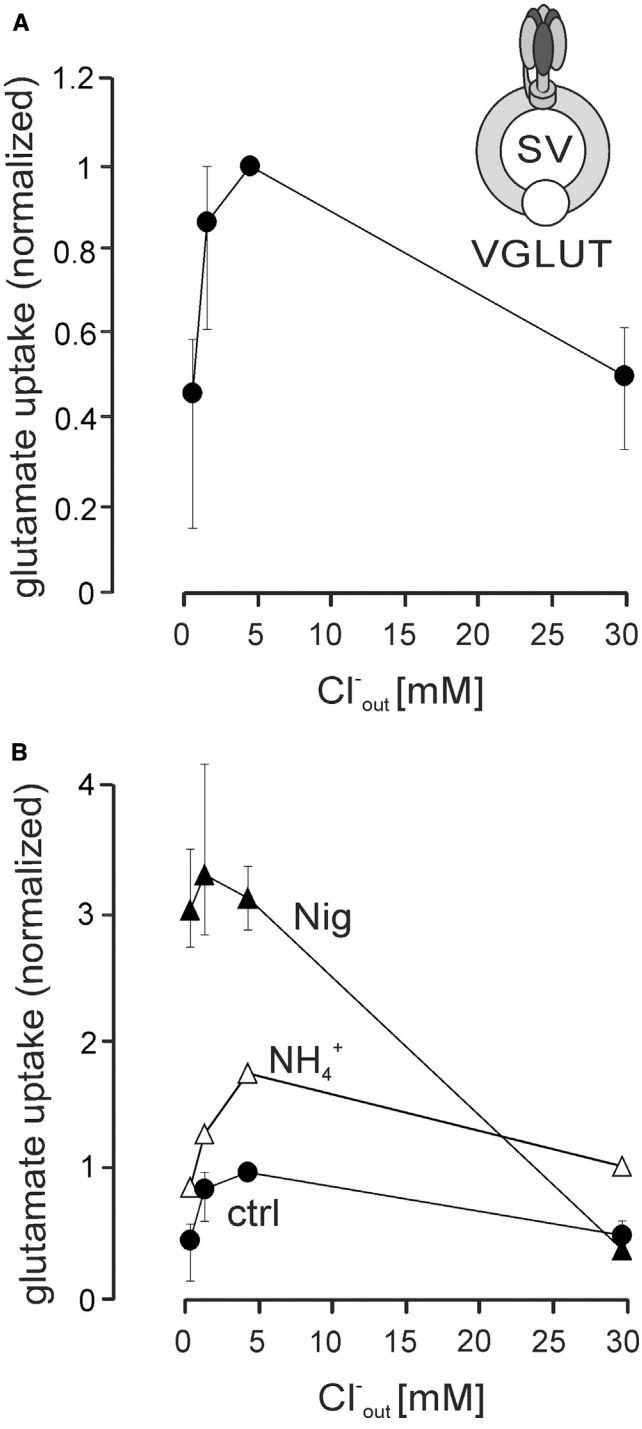

Figure 1. Cl^- Dependence of Glutamate Uptake by Isolated Synaptic Vesicles in the Presence of Agents Dissipating ΔpH

(A) Chloride dependence of vesicular glutamate uptake was measured in K-gluconate uptake buffer supplemented with the given chloride concentrations. To keep osmolarity constant, chloride concentration was adjusted by substituting gluconate for chloride. Data are normalized to glutamate uptake at 4–5 mM chloride.*

(B) Glutamate uptake in the presence of 500 nM nigericin (Nig) or 10 mM $(NH_4)_2SO_4$ (NH_4^+) at varying external chloride concentrations was measured and normalized as in (A). In all experiments, ~10 μg LP2 was used per data point.*

Asterisk indicates mean values, with bars representing the experimental range; n = 5 (A), n = 3 (B, Nig), and n = 1 (B, NH_4^+). See also Figure S1.

underlying mechanisms. This is mainly due to the fact that it is experimentally challenging to differentiate the effect of chloride ions on the electrochemical proton gradient $\Delta\mu H^+$ from that on the transport cycles of the transporters. It has been known for many years that increasing external chloride concentrations results in a shift from $\Delta\psi$ to ΔpH, as chloride serves as a net counter-ion for the electrogenic proton import (Johnson, 1988; Maycox et al., 1990), probably entering the vesicle via ClC3. It is far less clear how chloride ions are involved in neurotransmitter and particularly glutamate uptake. Using co-reconstitution of purified transporters with a eubacterial F_oF_1 ATPase, VGLUT1 was reported to operate as solute-chloride exchanger (Schenck et al., 2009). However, the notion that the VGLUT transport cycle is associated with net chloride flux has recently been challenged (Juge et al., 2010; Martineau et al., 2013).

Moreover, glutamate uptake is activated by low concentrations of chloride (Ahnert-Hilger et al., 2003; Naito and Ueda, 1985), which was attributed to an allosteric binding site on the cytoplasmic surface of the transporter (Hartinger and Jahn, 1993; Juge et al., 2010; Wolosker et al., 1996). Last but not least, it needs to be borne in mind that before being loaded with neurotransmitter, freshly endocytosed SVs are likely to be in equilibrium with the extracellular fluid, i.e., contain more than 120 mM NaCl in their lumen, whereas the cytoplasmic chloride concentration is probably considerably lower and depends on the neuron type.

Here we have used a combination of purified SVs, SVs fused with large liposomes containing an exogenous F_oF_1-ATPase, and liposomes co-reconstituted with purified VGLUT1 and F_oF_1-ATPase to clarify how SV are filled with glutamate while maintaining ionic, charge, and pH balance. Our data suggest that VGLUT possesses at least one cation and two independent anion binding sites, one of which prefers glutamate and one chloride ions, which together explain that in addition to the proton pump, no other components except VGLUT are required for efficient glutamate uptake.

RESULTS

The Role of Chloride in the Vesicular Transport of Glutamate

First, we used SVs purified from rat brain to revisit the effect of varying Cl^- concentrations on vesicular glutamate uptake (Figure 1A). In agreement with previous publications (Hell et al., 1990; Juge et al., 2006; Naito and Ueda, 1985; Winter et al., 2005), glutamate uptake was strongly activated by low chloride concentrations, peaking around 4 mM, and then declined (Figure 1A). Since an increase in the chloride concentration is associated with a shift from $\Delta\psi$ to ΔpH (El Mestikawy et al., 2011; Johnson, 1988; Tabb et al., 1992; Xie et al., 1983), we selectively dissipated the proton gradient either by nigericin or by ammonium sulfate. Nigericin is an electroneutral cation exchanger that exchanges H^+ against K^+, resulting in alkalinisation of the

lumen. Nigericin strongly increased glutamate uptake at low chloride concentrations (Figure 1B), an effect that can probably be attributed to a compensatory increase in $\Delta\psi$ (Henderson, 1971; Tabb et al., 1992). A similar but less pronounced stimulation was observed when the pH gradient was dissipated by ammonium sulfate, which is based on an equilibration of membrane-permeant NH_3 that captures protons in the lumen and equalizes the free proton concentration on both sides of the membrane (Henderson, 1971). In both conditions, VGLUT activity declined again at higher chloride concentrations, in agreement with earlier reports (Tabb et al., 1992; Wolosker et al., 1996). There are two possible explanations for this decline. First, it is conceivable that the membrane potential is reduced at high chloride due to a charge-compensating influx of chloride, which due to the clamping of the lumenal pH would result in a reduction of the driving force $\Delta\mu H^+$. Such influx may be mediated by the chloride-proton exchanger ClC3 that is probably present on synaptic vesicles (Jentsch et al., 1999; Stobrawa et al., 2001). However, no difference in the biphasic chloride dependence was observable when synaptic vesicles were isolated from the brain of ClC3-KO mice (see Figure S1A available online). Second, it is possible that chloride directly competes with glutamate for uptake, which will be discussed further below.

We also examined whether the chloride dependence of VGLUTs varies with the VGLUT isoform. This, however, was not the case: very similar data were obtained when SVs from VGLUT1-KO mice were used, although the overall activity was lower (Figure S1A). In these mice, the remaining transport activity is contributed mainly by VGLUT2. Furthermore, there is no difference in the chloride effects between SV immunoisolated with VGLUT1- or VGLUT2-specific antibodies, respectively (Figure S1B).

To fully understand the role of chloride in VGLUT-mediated glutamate transport, it is necessary to control the chloride concentration not only on the cytoplasmic but also on the lumenal face of the vesicles. To this end, we reconstituted recombinant VGLUT1 purified from insect cells with a recombinant purified F_oF_1-ATPase derived from the thermophilic Bacillus PS3 (TF_oF_1) in liposomes (Figures 2A and S2A), i.e., using an approach similar to that used previously by Schenck et al. (2009) and Juge et al. (2006). Here both lumenal and external ionic conditions can be separately controlled, and contributions by other ion channels or ion exchangers present on SVs can be excluded.

First, we determined the orientation of VGLUT1 after reconstitution by incubating the liposomes with TEV-protease. VGLUT contains a streptavidin binding peptide tag (~5 kDa) on the cytoplasmically oriented N terminus that is only accessible to the protease if the transporter is in the correct orientation. Upon protease incubation, almost all VGLUT1 exhibited a slight reduction in size which was comparable to that observed after detergent treatment, indicating that the transporter is predominantly inserted in the correct orientation (Figure S2B). Next we checked whether the F_oF_1-ATPase is capable of generating a stable electrochemical proton gradient under our experimental conditions. Liposomes were equilibrated with 150 mM K-gluconate on both sides of the membrane. As shown in Figure 2B, a large inside-positive membrane potential develops upon addition of ATP (Figure 2B), which is due to the electrogenic transport of protons in the absence of counter-ion conductance. When the K^+-ionophore valinomycin was added, the membrane potential collapsed due to the charge-neutralizing efflux of K^+ ions (Figure 2B), allowing the ATPase to pump in protons and generate a stable pH gradient (Figure 2C). These data demonstrate that the reconstituted system is energetically tightly coupled.

We then used this system to investigate the chloride dependence of glutamate transport. Liposomes containing both VGLUT1 and TF_oF_1 exhibited a robust uptake of glutamate that was dependent on ATP and sensitive to FCCP and to the VGLUT-specific inhibitor Evans blue (Figure 2D). In these experiments, the liposomes contained 300 mM glycine. Again, these liposomes exhibited a biphasic chloride dependence with a peak around 5 mM, closely resembling the chloride dependence of glutamate uptake by purified SVs. We then prepared liposomes containing encapsulated choline chloride (150 mM). In the absence of external chloride, uptake was strongly increased over the glycine control (Figure 2E). When the external chloride concentration was increased, we again observed a strong decline at high chloride concentrations. Intriguingly, we did not observe a consistent activation at low external chloride concentrations, although there was some variability between individual experiments. When liposomes were preloaded with choline gluconate, the results were very similar to those obtained with glycine-loaded liposomes (data not shown), excluding nonspecific salt effects on the transport rate.

Together, we conclude that VGLUT-mediated transport is profoundly enhanced by chloride inside the vesicle in a manner that is superimposed to the activation by chloride at the cytoplasmic side. These effects can only be attributed to VGLUT itself, as TF_oF_1 shows no chloride dependence (Schenck et al., 2009) (data not shown). Consequently, the regulatory chloride binding site appears to be accessible to both faces of the membrane during the transport cycle. Such a scenario suggests that in the presence of a chloride concentration, gradient net transport of chloride ions may occur. To examine whether this is the case, we used two independent approaches. First, we tested whether in the presence of an inwardly directed chloride gradient (and low lumenal buffering capacity), ATP-dependent acidification is observable. This was indeed the case (Figure 2F), although some leakage was also observed (reduced but measurable acidification in the absence of VGLUT). Second, we prepared VGLUT1 liposomes loaded with 150 mM KCl and the chloride sensitive fluorescent probe 6-methoxy-*N*-(3-sulfopropyl)quinolinium (SPQ) (Biwersi et al., 1994; Verkman, 1990), which is quenched at high chloride concentrations. When these liposomes were incubated in an osmotically equivalent external potassium gluconate buffer, addition of valinomycin induced dequenching that was dependent on the presence of VGLUT1 (Figure 2H). No dequenching was observable when the outwardly directed chloride concentration gradient was abolished (replacement of gluconate with chloride) (Figure 2I). These observations confirm the previous notion that chloride translocation is an intrinsic property of VGLUTs (Schenck et al., 2009), as no other chloride channel or transporter is present. The chloride translocation activity is not or is only loosely coupled to glutamate transport, as chloride-induced acidification was observable in the absence of glutamate but can be partially overcome by adding glutamate (Figure 2G).

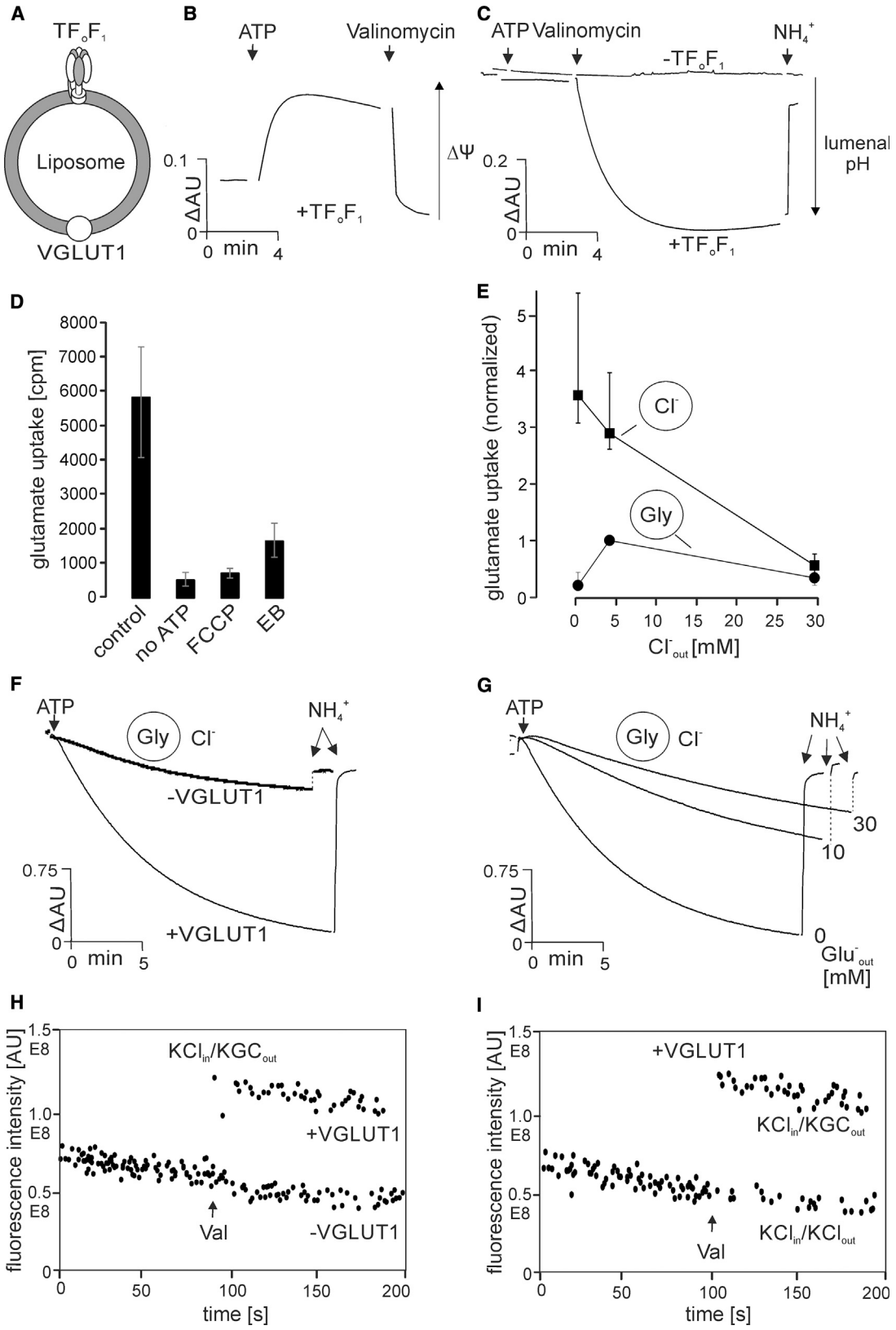

(legend on next page)

While reconstitution of purified components represents the cleanest system for analyzing ion dependence of the transporter, it cannot be excluded that the properties of the transporter are different when maintained in its native environment. For these reasons, we established an experimental approach in which large liposomes containing the TF_oF_1-ATPase are fused with purified synaptic vesicles. In this system, all endogenous proteins are present in the correct orientation. To this end, we took advantage of a SNARE-dependent fusion system developed earlier in our laboratory that allows for fast and highly efficient fusion between native synaptic vesicles and liposomes containing a stabilized SNARE acceptor complex (Holt et al., 2008) (see cartoon in Figure 3A). We have shown previously that hybrid vesicles are nonleaky (van den Bogaart et al., 2010), and since we used liposomes with an average diameter of 100 nm (2.5 times the diameter of SVs, i.e., more than 10-fold higher volume [Hernandez et al., 2012]), the final lumenal buffer and ion composition can be effectively controlled by this procedure. To exclude interference by unfused SV, the endogenous V-ATPase was inactivated by bafilomycinA1 so that glutamate uptake by the endogenous VGLUTs can only be driven by fused SV containing the exogenous TF_oF_1-ATPase (Figure 3A).

The resulting hybrid vesicles displayed robust chloride-dependent acidification when low lumenal buffer concentrations were used (Figure 3B, see above), with even less leakage than observed in the reconstituted system (compare Figure 2F). Acidification was slower than that of native SVs (data not shown), most likely due to the larger volume.

Glutamate uptake of fused SVs was dependent on the presence of ATP and TF_oF_1 and sensitive to FCCP (Figure 3C). When liposomes were loaded with chloride instead of gluconate before fusion, uptake was enhanced about 3-fold (Figure 3D). Glutamate uptake was stimulated by chloride from the outside regardless of whether chloride ions were also encapsulated inside or not, confirming that chloride ions activate VGLUT directly by occupying one or several binding sites that are accessible both from the cytoplasmic and the lumenal side during the transport cycle.

As in the experiments using either purified SVs or purified reconstituted proteins, we again observed a strong decline of uptake when the chloride concentration was raised above the optimum around 5 mM. Based on a suggestion by Bellocchio et al. (2000), we therefore explored the possibility that in addition to acting on a regulatory binding site, chloride may also directly compete with glutamate for uptake at high concentrations. Indeed, a rather profound inhibition of chloride-dependent acidification by glutamate was observable (Figure 3E). These data suggest (1) that chloride-dependent acidification of synaptic vesicles is, at least in part, mediated by chloride transport via VGLUT, and (2) that chloride is able to bind to the substrate binding site in a competitive manner.

Binding and Transport of Monovalent Cations by VGLUT

As discussed in the introduction, an exit pathway for protons is required for efficient loading of synaptic vesicles with glutamate. Recently, a cation/proton exchange activity has been found on SVs (Goh et al., 2011). In this work, addition of monovalent cations was found to reduce acidification and to stimulate glutamate uptake by shuttling lumenal protons for external cations. The activity was attributed to a sodium proton exchanger of the NHE family, largely based on its inhibition by the NHE-specific drug EIPA (ethyl-isopropyl amiloride). Furthermore, it was shown directly that SV can sequester externally added ^{22}Na (Goh et al., 2011).

Indeed, we identified the cation/proton exchanger NHE6 by western blotting on highly purified SVs (Figure S3). Furthermore, we observed that in the presence of ATP, glutamate-dependent acidification is largely reversed upon addition of K^+ and to a slightly lower extent by Na^+, but only weakly by the membrane impermeable monovalent cation choline (Figure 4A). Accordingly, glutamate uptake was stimulated in the presence of K^+ (Figures 4B and 4C) and Na^+ (Figure 4D). The chloride dependence of glutamate transport in the presence of K^+ showed the strongest stimulation at 0 mM chloride decreasing at higher chloride concentrations (Figure 4C). Na^+ enhanced glutamate uptake at higher chloride concentrations (Figure 4D), all in agreement with Goh et al. (2011). However, in our hands the NHE inhibitor EIPA (ethyl-isopropyl amiloride) did not reverse the promoting effect of either Na^+ or K^+ (Figure 4B; data not shown).

To shed more light on the mechanism by which these cations activate glutamate transport, we used our hybrid system (SVs

Figure 2. Dependence of Glutamate Uptake on Internal and External Cl^- Using Proteoliposomes Reconstituted with Purified VGLUT1 and TF_oF_1

(A) (Left) Diagram of proteoliposomes containing purified recombinant VGLUT1 and the proton ATPase TF_oF_1.

(B and C) Changes in membrane potential (B) and ΔpH (C) generated by the TF_oF_1 ATPase, measured with the dyes OxonolVI and acridine orange, respectively. Proteoliposomes containing TF_oF_1 were preloaded with 150 mM K-gluconate and incubated in the same buffer. Proton pumping resulted in the development of an inside positive membrane potential ($\Delta\psi$) that was dissipated by the K^+-ionophore valinomycin due to charge compensation, resulting in net inward transport of protons and acidification. The proton gradient was then dissipated by addition of $(NH_4)_2SO_4$ (NH_4^+).

(D) Glutamate uptake by proteoliposomes reconstituted with both TF_oF_1 and VGLUT1, measured at 4 mM choline chloride and 150 mM choline gluconate, in the presence (control) or absence of ATP (no ATP), FCCP, and 1 μM Evans blue (EB). VGLUT1 (6–8 μg) was assayed per measurement.*

(E) Chloride dependence of ATP-induced glutamate uptake using proteoliposomes preloaded with either 300 mM glycine (Gly) or 150 mM choline chloride (Cl^-), using conditions as in (D). The data were normalized to uptake at 4 mM Cl^-_{out} and no chloride inside (Gly).*

(F) ATP-dependent acidification of proteoliposomes containing TF_oF_1 in the presence or absence of VGLUT1. Liposomes were preloaded with 300 mM glycine (Gly), and acidification was measured in 30 mM external choline chloride (Cl^-) using acridine orange as reporter dye (ΔAU, changes in absorption).

(G) Acidification of VGLUT1/TF_oF_1 liposomes in the presence of 30 mM external chloride (Cl^-) and 0, 10, and 30 mM external glutamate (Glu^-_{out}).

(H and I) Chloride efflux from VGLUT1 liposomes was monitored using 6-Methoxy-*N*-(3-sulfopropyl)quinolinium (SPQ) as a chloride-sensitive fluorescent probe. SPQ dequenching upon addition of 2 nM valinomycin (Val) was measured in (H) ± VGLUT1 liposomes preloaded with 150 mM KCl/30 mM K-gluconate and SPQ in the presence of 180 mM external K-gluconate (KCl_{in}/KGC_{out}). (I) +VGLUT1 liposomes preloaded with 150 mM KCl/30 mM K-gluconate and SPQ at either 180 mM external K-gluconate (KCl_{in}/KGC_{out}) or 150 mM KCl/30 mM K-gluconate (KCl_{in}/KCl_{out}).

Asterisk indicates mean values, with bars representing the experimental range; n = 3 (D), n = 5 (E, Gly), and n = 4 (E, Cl^-). See also Figure S2.

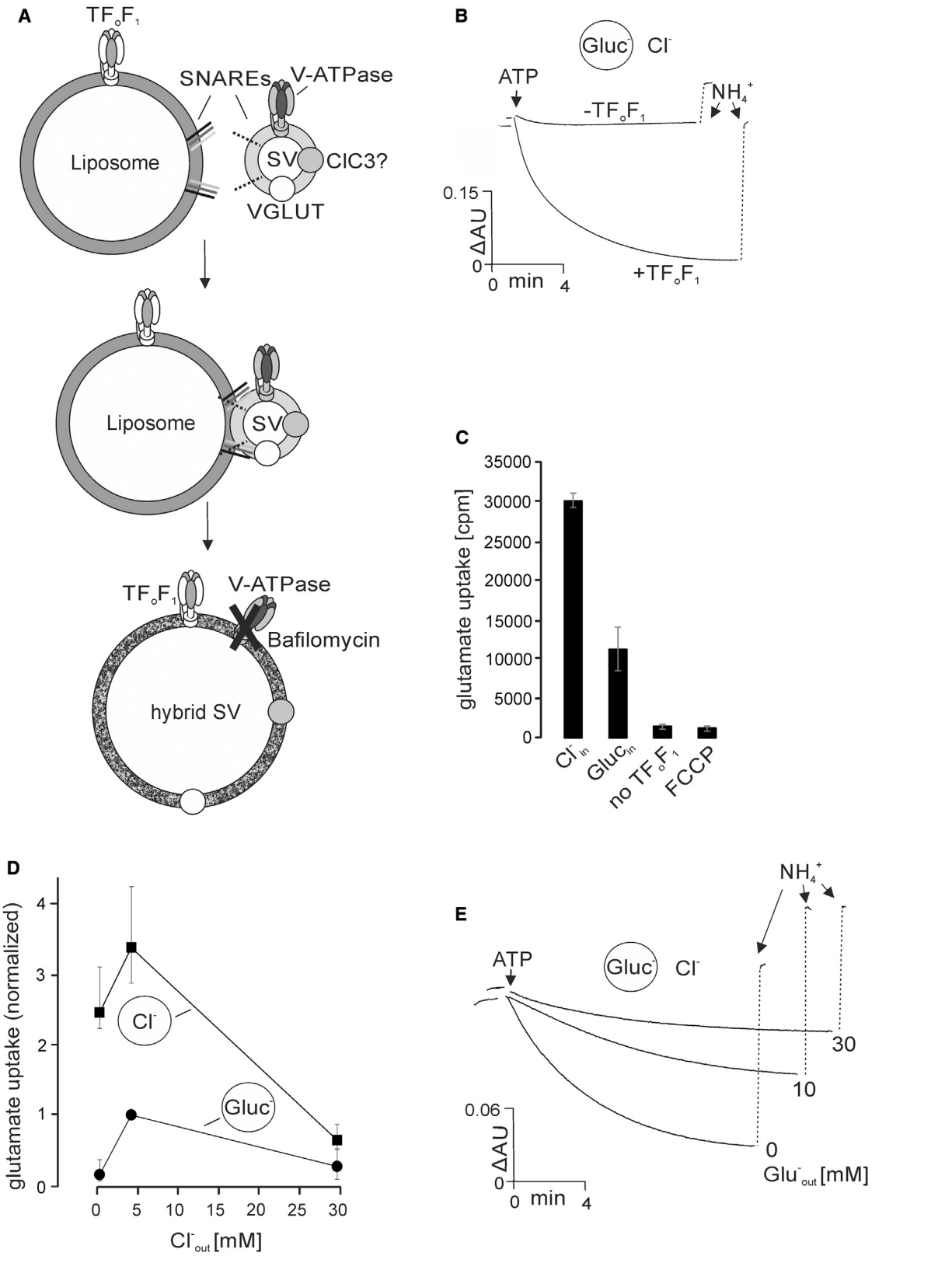

(legend on next page)

fused to TF_oF_1-containing liposomes, see Figure 3A) to measure glutamate uptake at varying external and lumenal chloride concentrations in the absence and presence of K^+ or Na^+ ions. At 0 mM external chloride, K^+ increased glutamate uptake ~2.5-fold, while Na^+ evoked only minor changes (Figures 5A and 5B). However, when the hybrid SVs were preloaded with 150 mM chloride, the K^+-induced stimulation at low external chloride was less pronounced (Figure 5C), most likely being partially masked by the strong stimulatory effect of lumenal chloride. The stimulatory effect of K^+ decreased at higher external chloride concentrations (Figures 5B and 5C), irrespective of whether the lumen contained chloride or not. This is surprising, since K^+ reversed ΔpH at 30 mM extralumenal chloride (data not shown). We conclude that inhibition of glutamate uptake at 30 mM chloride is independent of ΔpH. As discussed above, this is probably due to a competition between chloride and glutamate that becomes apparent at high chloride concentrations. Furthermore, subsequent addition of K^+, nigericin, and NH_4^+ leads to a stepwise increase of $\Delta\Psi$ in fused SVs (Figures S4A and S4B), corroborating that the mechanism underlying glutamate uptake stimulation by K^+ is affecting $\Delta\mu H^+$.

Taken together, our findings confirm the presence of a K^+/H^+ exchange activity that depletes ΔpH and increases $\Delta\Psi$. Since NHEs do not appear to be responsible, we investigated whether the activity may be mediated by a cation binding site of VGLUT itself. VGLUT has been invoked previously in coupled cation transport, both upon conditions of high ΔpH as well as in its "second life" as a Na^+-coupled phosphate transporter (Aihara et al., 2000; Ni et al., 1994).

In order to test whether VGLUT itself may be responsible for the K^+-induced effects on glutamate uptake, we used our minimal reconstituted system containing purified VGLUT1 and TF_oF_1. Indeed, glutamate uptake was enhanced more than 2-fold in the presence of K^+ when chloride was absent, with the stimulatory effect again decreasing at higher external chloride concentrations (Figures 6A and 6B). Again, preloading of the VGLUT1 liposomes with 150 mM lumenal chloride decreases the stimulatory effect of K^+ (Figure 6C), and no stimulation was observed with Na^+ (Figure 6A). Thus we conclude that the K^+-dependent enhancement of glutamate uptake is due to a direct interaction of K^+ ions with the VGLUT protein. Interestingly, the VGLUT-specific inhibitor Evans blue blocked K^+-induced, but not Na^+-induced, alkalinization of SVs (Figures S5A and S5B), suggesting that the Na^+-dependent effect on alkalinization may be due to a different protein, with vesicular NHE6 being a good candidate. Note that neither chloride- nor glutamate-dependent acidification was inhibited by Evans blue (Figures S5A and S5B; data not shown), suggesting that Evans (and trypan) blue inhibits VGLUT by interfering with the cation rather than the anion binding site despite its multiple negative charges. Correspondingly, nigericin reverses the inhibitory effect of Evans and trypan blue on glutamate uptake in a dose-dependent manner (Figure S5C; data not shown). To shed more light on the unexpected discrepancy between uptake and acidification, we carried out a dose-response experiment with Evans blue (Figure S5D). Even under saturating conditions, glutamate uptake is not completely inhibited (Figure S5D), raising the possibility that the block may also be reverted by the much higher substrate concentrations used in acidification experiments. Intriguingly, similar to the cytosolic K^+ selectivity found in VGLUT, a monovalent cation selectivity was previously reported for excitatory amino acid transporters (EAATs) on the plasma membrane, which are coupling glutamate transport to the inwardly directed Na^+ gradient and to the outwardly directed K^+ gradient (Danbolt, 2001; Ryan and Mindell, 2007; Vandenberg and Ryan, 2013). However, in contrast to EAATs, glutamate uptake was not affected by an outwardly directed Na^+ gradient measured in hybrid SVs and VGLUT liposomes preloaded with either Na-gluconate or NaCl (data not shown).

To further assess the role of VGLUT in K^+-dependent glutamate, we used light membrane fractions of PC12 cells heterogeneously expressing VGLUT2 (VGLUT2-LMFs). PC12 cells are naturally devoid of VGLUTs, allowing for measuring changes in glutamate uptake solely mediated by VGLUT in the presence of a native V-ATPase. We were able to measure FCCP-sensitive VGLUT2-specific glutamate uptake, while the light membrane fractions isolated from control cells did not accumulate glutamate (Figure 7A; data not shown). Strikingly, similar to our findings on reconstituted liposomes, we measured K^+-stimulated glutamate uptake in VGLUT2-LMFs, which was strongest at 0 mM chloride and dissipated at 30 mM chloride (Figure 7B). These data further corroborate VGLUT's capability to mediate K^+ enhancement of glutamate uptake. Stimulation of glutamate uptake in the presence of the K^+/H^+ exchanger nigericin showed a corresponding pattern in VGLUT2-LMFs (Figure 7B) and in SVs (Figure 1B), suggesting that VGLUTs operate in a similar K^+/H^+ exchanging manner. Notably, the stimulatory effect on glutamate uptake was again selective to K^+ and was not measured with Na^+ (Figure 7A), supporting the view that the transporter,

Figure 3. Glutamate Uptake by Hybrid Vesicles Resulting from the Fusion of Synaptic Vesicles with TF_oF_1-Containing Liposomes: Dependence on Internal and External Cl^-

(A) Diagram showing the formation of hybrid vesicles. TF_oF_1 liposomes containing an activated Q-SNARE acceptor complex were fused with native SVs containing the endogenous R-SNARE synaptobrevin. The endogenous V-ATPase was inhibited by 0.2 μM bafilomycinA1, making glutamate uptake solely dependent on the external TF_oF_1-ATPase.

(B) Acidification hybrid vesicles preloaded with 150 mM choline gluconate ($Gluc^-$) were monitored in the presence and absence of TF_oF_1 at 30 mM external choline chloride and 0.2 μM bafilomycinA1. Hybrid SVs showed a strong chloride-dependent acidification that was dependent on the presence of TF_oF_1.

(C) Glutamate uptake by hybrid vesicles preloaded with either 150 mM choline gluconate ($Gluc^-$) or 150 mM choline chloride (Cl^-). The assay was performed at 4 mM external choline chloride and 150 mM choline gluconate in the presence of 0.2 μM bafilomycin A1 (~15 μg of total protein/data point).*

(D) Cl^- dependence of glutamate uptake by hybrid vesicles that were preloaded with 150 mM choline gluconate ($Gluc^-$) or choline chloride (Cl^-). Assay conditions were as in (C).

(E) Inhibition of chloride-dependent acidification by glutamate. Hybrid vesicles were loaded with 150 mM choline gluconate ($Gluc^-$), and acidification was monitored in the presence of 30 mM external choline chloride (Cl^-) in the absence or presence of glutamate (Glu^-_{out}) at the indicated concentrations.

Asterisk indicates mean values, with bars representing the experimental range. n = 3 (C), n = 6 (D, Cl^-), and n = 4 (D, $Gluc^-$).

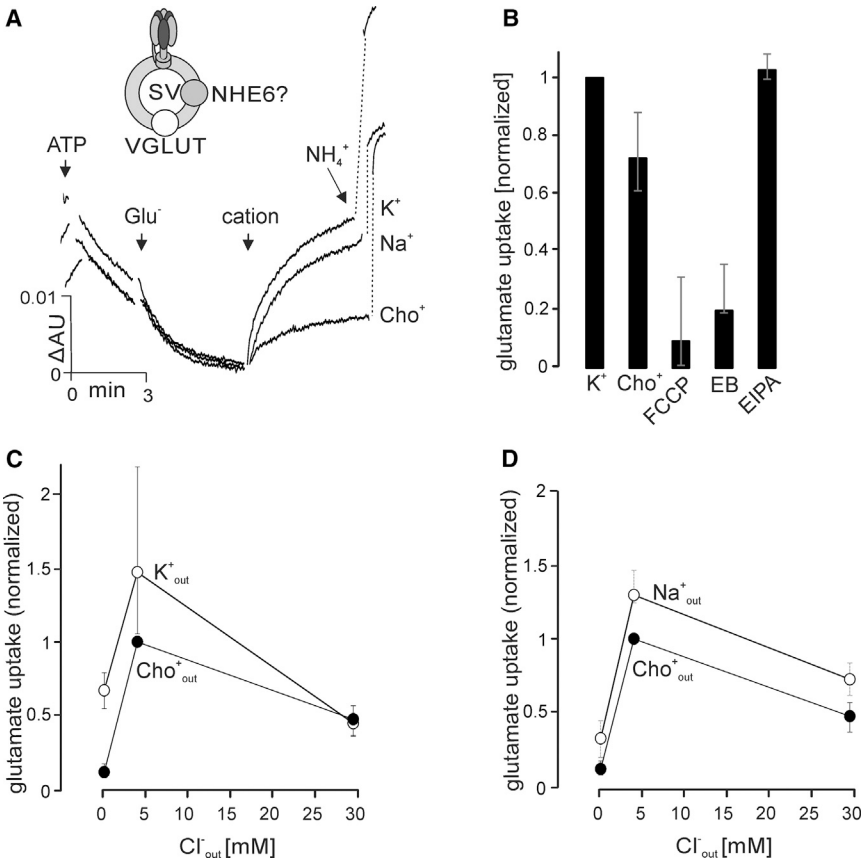

Figure 4. Effects of Monovalent Cations on ΔpH and on Glutamate Uptake by Synaptic Vesicles

(A) Changes in ΔpH upon sequential addition of ATP, glutamate (Glu^-), and K^+, Na^+, and choline (Cho^+) (gluconate salts, all at a final concentration of 30 mM) (SV fraction). See Figure 2 for details.

(B) Influence of monovalent cations and of inhibitors on glutamate uptake by SVs (LP2 fraction). The additions were K-gluconate (K^+) and choline gluconate (Cho^+) (both 50 mM). Both the protonophore FCCP (30 μM) and the VGLUT-specific inhibitor Evans blue (EB, 10 μM) inhibited uptake. In contrast, EIPA, an inhibitor of Na^+/H^+ exchangers (at 50 μM), had no effect. All measurements were carried out at an external chloride concentration of 4 mM. Data are normalized to the glutamate uptake with K^+.*

(C and D) Glutamate uptake by SVs (LP2-fraction) in 50 mM K-gluconate (C) or 50 mM Na-gluconate (D) in dependence on the external Cl^- concentration (Cl^-_{out}). As control, uptake was measured in the presence of the membrane-impermeant cation choline (Cho^+_{out}, 50 mM choline gluconate). Data were normalized to uptake in the presence of Cho^+_{out} at 4 mM Cl^-.*

Asterisk indicates mean values, with bars representing the experimental range; n = 3 (B), n = 4–5 (C, K^+_{out}), n = 5 (C, Cho^+_{out}), n = 4–5 (D, Na^+_{out}), and n = 5 (D, Cho^+_{out}). See also Figure S3.

at least when accessed from the cytoplasmic face, is selective for potassium ions.

DISCUSSION

In the present study we used a combination of different approaches to show that VGLUT, in addition to its capacity to transport glutamate, displays a chloride transport mode and a K^+/H^+ antiport mode, which are apparently only loosely coupled to glutamate transport. These properties enable VGLUT to maximize glutamate uptake while adjusting to the changing ionic environment during transport. Our findings can be integrated into a model according to which the transporter possesses two anion binding sites, one of which binds chloride and the second of which preferentially binds glutamate, and at least one cation binding site with cytosolic preference of K^+ over Na^+ and lumenal binding of H^+ (Figure 8).

In recent years, major progress has been made concerning the structural and functional understanding of solute carriers. In particular, it is becoming apparent that despite their diversity, bacterial transporters (and by analogy probably also their eukaryotic relatives) are structurally highly conserved (Krishnamurthy et al., 2009). Most of the sodium and proton gradient-coupled transporters can be classified in only two main folds which comprise the LeuT fold, a eubacterial ortholog of transporters for positively charged and neutral neurotransmitters such as glycine, GABA, and monoamines, and the GltPh fold, the archebacterial ortholog of transporters for the negatively charged neurotransmitters glutamate and aspartate (Focke et al., 2013; Gouaux, 2009; Krishnamurthy et al., 2009). Based on these similarities, it is legitimate to extrapolate to eukaryotic transporters including VGLUTs, in particular with respect to the understanding of the ion and substrate binding sites and the conformational transitions during transport.

Figure 8 shows a model for the VGLUT transport cycle under two different conditions, which builds on these developments and tries to integrate our present knowledge about chloride regulation and K^+/H^+ antiport, both from this work and from previous publications (Bellocchio et al., 2000; Goh et al., 2011; Hartinger and Jahn, 1993; Juge et al., 2006, 2010; Maycox et al., 1988; Naito and Ueda, 1985; Schenck et al., 2009; Tabb et al., 1992; Takamori et al., 2000; Wolosker et al., 1996). It is based on the following assumptions: analogous to all transporters crystallized so far (including GltPh and LeuT), we assume that the transporter shuttles between two main conformations in which the substrate binding pocket is open either at the cytoplasmic (state I) or the lumenal side (state II, see Figure 8) (Rudnick, 2011). We assume further that the hydrophilic binding pocket contains at least three ion binding sites: two for anions and at least one for monovalent cations. Of the anion binding sites, one is specific for Cl^- with an affinity in the low mM range, suggesting that it is always occupied under physiological conditions and does not result in net Cl^- transport (referred to as Cl^- binding site). The second anion binding site is responsible for substrate

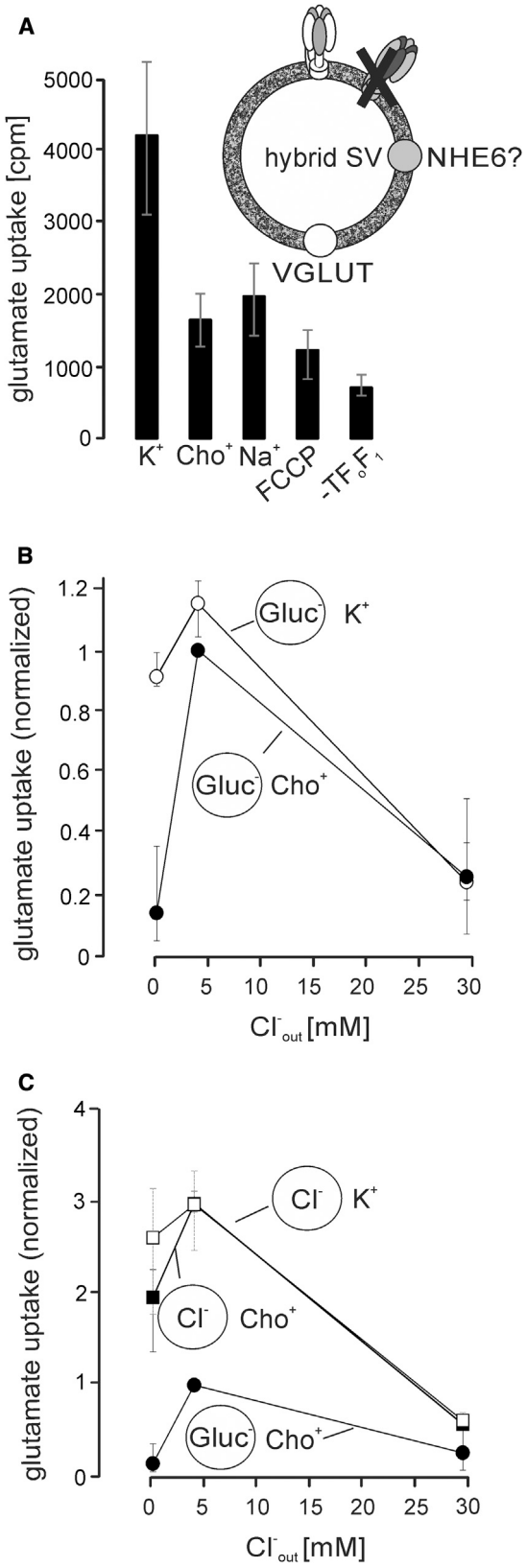

Figure 5. K^+ Stimulates Glutamate Transport by Hybrid Vesicles

(A) Glutamate uptake by hybrid vesicles preloaded with 150 mM choline gluconate was measured in the absence of external Cl^-. The additions were K-gluconate (K^+), Na-gluconate with 100 μM TBOA (Na^+), or choline gluconate (Cho^+), all at 50 mM, and FCCP (30 μM). A control included hybrid vesicles generated by fusion with liposomes lacking TF_oF_1 (-TF_oF_1).*

(B and C) Cl^- dependence of glutamate uptake by hybrid vesicles that were preloaded either with 150 mM choline gluconate ($Gluc^-$) (B) or with 150 mM choline chloride (Cl^-) (C) in the presence of 50 mM K-gluconate (K^+) and choline gluconate (Cho^+). Data were normalized to the glutamate uptake in the presence of Cho^+ and 4 mM Cl^-_{out}.*

Asterisk indicates mean values, with bars representing the experimental range; n = 3 (A), n = 3 (B, K^+), n = 6 (B, Cho^+), n = 3 (C, K^+), n = 3 (C, Cho^+), and n = 6 (C, $Gluc_{in}$ Cho^+_{out}). Also see Figure S4.

binding. It prefers glutamate (thus referred to as Glu^- binding site) but also binds Cl^-, albeit with lower affinity. At present, we do not know whether these sites influence each other.

While the transporter can switch from state I to state II with only the glutamate binding site being occupied, conformational switching is accelerated when the chloride binding site is also occupied. In state II, the affinity for glutamate is low, resulting in dissociation, whereas either the affinity or the dissociation rate constant of chloride to this site is not reduced in a similar manner. Reversal from state II to state I is also accelerated when the chloride binding site is occupied, suggesting that chloride binding may lower the activation energy for the conformational transition in either direction. This is supported by the finding that chloride activation is maximal when chloride is present on both sides of the membrane.

The cation binding site appears to show a strong preference for K^+ ions in state I. Furthermore, our data suggest that protons can be transported in the reverse direction, resulting in a K^+/H^+ exchange activity that, however, does not appear to be tightly coupled, at least not to glutamate transport. This antiport of a lumenal proton and a cytosolic potassium converts lumenal ΔpH into Δψ, while conformational switching is presumably not accelerated, as the kinetics of glutamate transport are not affected by the cations (Goh et al., 2011).

The presence of ion binding sites whose occupancy is not directly coupled to the conformational transition endows the transporter with a high degree of flexibility, allowing for an adjustment to the changing ionic environment during transport. After exocytosis, synaptic vesicles are re-endocytosed and thus contain extracellular fluid, including NaCl well above 100 mM and buffers with a capacity in the range of 55–65 mM (Alpern et al., 1983; Deitmer and Rose, 1996; Goldsmith and Hilton, 1992). Under these conditions, the glutamate binding site is loaded with glutamate at the cytoplasmic face, while the cation binding may be at least partially occupied by K^+ (Figure 8B). Notably, the stimulatory effect of potassium is strongest in the absence of chloride, suggesting that, in addition to serving as a cation exchanger, this site may also activate the transporter when the chloride site is not occupied. After conformational switching, glutamate dissociates. Probably, the glutamate binding site is then at least partially occupied by Cl^-, as during this phase of transport the lumenal Cl^- concentration is much higher than that of glutamate, resulting in substoichiometric reverse transport of Cl^-. For maintaining osmotic balance it was

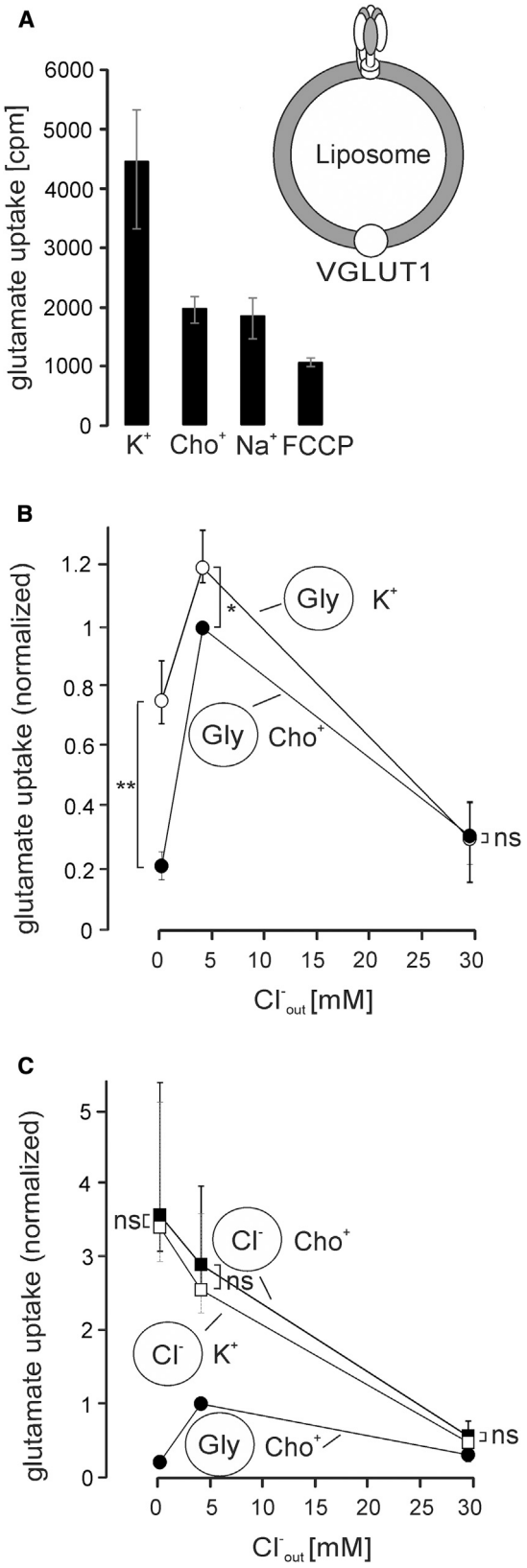

Figure 6. Stimulatory Effect of K^+ on Glutamate Uptake Is Mediated by VGLUT

(A) Glutamate uptake by VGLUT1/TF_oF_1 liposomes preloaded with 300 mM glycine was measured in the absence of external chloride. K-gluconate (K^+), Na-gluconate (Na^+), and choline gluconate (Cho^+) were present at 50 mM.*

(B and C) Cl^- dependence of glutamate uptake by VGLUT1/TF_oF_1 liposomes that were preloaded with 300 mM glycine (Gly) (B) or 150 mM choline chloride (Cl^-) (C). The liposomes were incubated in the presence of either 50 mM K-gluconate (K^+) or choline gluconate (Cho^+). Data were normalized to the uptake in presence of 50 mM Cho^+ and 4 mM Cl^-_{out} and were analyzed using a two-tailed paired t test, *$p < 0.05$ ($p = 0.017$), **$p < 0.01$ ($p = 0.0015$), and ns (not significant, $p > 0.05$).*

Asterisk indicates mean values, with bars representing the experimental range; n = 3 (A), n = 4 (B and C). See also Figure S5.

suggested that vesicles contain a "gel matrix," mainly consisting of oligosaccharyl side chains of the protein SV2, that is capable of osmotic buffering (Reigada et al., 2003). Alternatively, osmotic balance may be maintained by a net efflux of NaCl. We cannot exclude that the cation binding site of VGLUT can be used to export Na^+, although we were unable to detect an effect of Na^+ on glutamate transport. Alternatively, Na^+ may exit using NHE6 (see below) or may remain inside as counter-ion for glutamate, being balanced by proton export or substoichiometric K^+/H^+ exchange via the cation binding site. Overall transport is electrogenic, with charge compensation being provided by pumping of H^+ that is neutralized by the entrapped buffers.

Ongoing transport results in an accumulation of glutamate inside the vesicle. Most importantly, the buffering capacity of the lumenal buffers will become exhausted, resulting in a net acidification of the vesicle lumen, requiring a proton exit pathway for continued transport once the lumenal pH reaches its steady-state value of ~5.5 (Füldner and Stadler, 1982; Michaelson and Angel, 1980; Nguyen and Parsons, 1995). These conditions are experimentally more difficult to access, as radiotracer uptake experiments cannot easily be carried out at the required high glutamate concentrations. However, under these conditions K^+/H^+ antiport mediated by the cation binding site is likely to play a major role in sustaining glutamate uptake as it maintains $\Delta\Psi$ and decreases ΔpH (Figure 8C). Furthermore, reverse transport of Cl^- ceases due to the reduction in the lumenal Cl^- concentration.

The model proposes a mechanism for glutamate transport which, in contrast to classical transporters such as plasma membrane neurotransmitter transporters, is not tightly coupled to the transport of other ions but rather engages the available anionic and cationic gradients for optimal loading of glutamate into the synaptic vesicle. It also reconciles, at least in part, the seeming contradictions between the study of Schenck et al. (2009), who reported a strong stimulation by lumenal chloride of glutamate uptake in a reconstituted system (which we have now corroborated), and the inability of Juge et al. (2010) to detect chloride uptake during glutamate uptake. Our data show clearly that Cl^- can be transported by VGLUT, as both chloride-dependent acidification and chloride efflux are observable in liposomes containing only TF_oF_1 and VGLUT. Furthermore, due to the interference by high concentrations of glutamate, we assume that chloride directly competes with glutamate binding, in agreement with a previous suggestion (Bellocchio et al., 2000). Thus, high cytoplasmic chloride not only enhances ΔpH at the expense of $\Delta\psi$

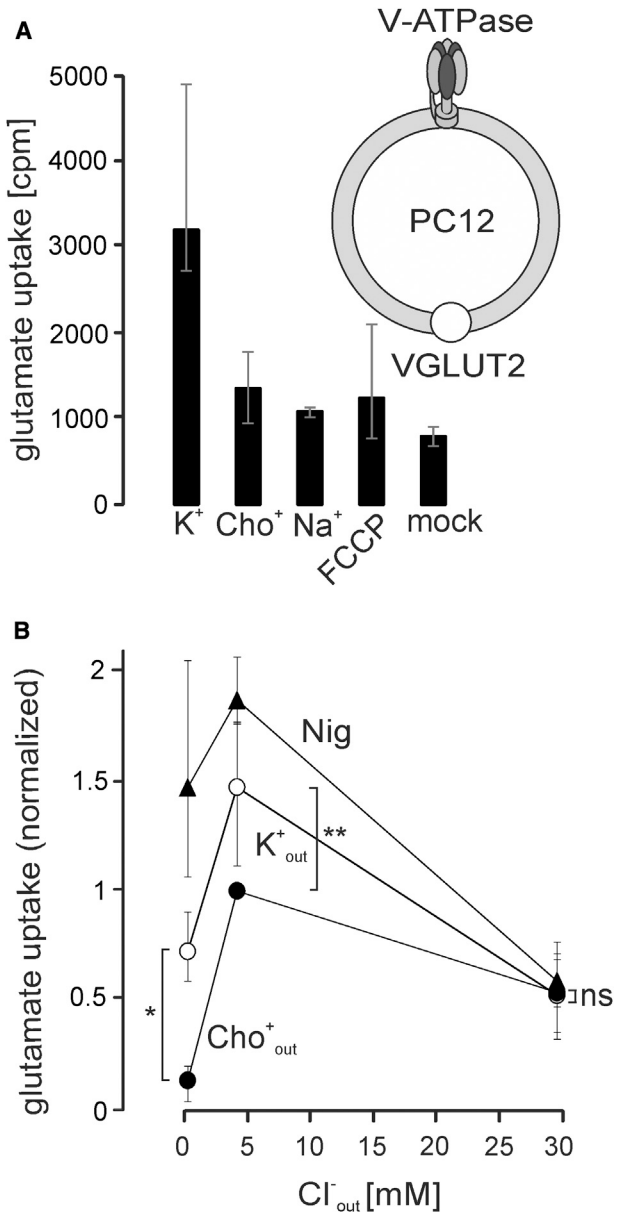

Figure 7. Membrane Vesicles Isolated from VGLUT2-Expressing PC12 Cells Show K^+ Stimulation of FCCP-Sensitive Glutamate Uptake

(A) Glutamate uptake by light membrane fractions isolated from PC12 cells stably expressing VGLUT2. The incubation conditions were as described in the legend to Figure 5A. Light membranes from mock-transfected PC12 were used as control.*

(B) Cl^- dependence of glutamate uptake. Uptake was measured in the presence of 50 mM K-gluconate (K^+_{out}) or choline gluconate (Cho^+_{out}). Nig, incubation in the presence of K-gluconate and nigericin (10 nM). The data were normalized to Cho^+_{out} and 4 mM Cl^-_{out} and analyzed using a two-tailed paired t test, *$p < 0.05$ ($p = 0.016$), **$p < 0.01$ ($p = 0.01$), and ns (not significant, $p = 0.7$).*

Asterisk indicates mean values, with bars representing the experimental range; n = 3 (A), n = 3 (B, Nig), n = 3–6 (B, K^+_{out}), and n = 3–6 (B, Cho^+_{out}).

but also directly interferes with glutamate transport, explaining the strong drop in glutamate uptake at high chloride concentrations (Bellocchio et al., 2000; Juge et al., 2006; Schenck et al., 2009; Tabb et al., 1992). The inability of Juge et al. to detect Cl^- inward transport during glutamate transport can be readily explained, because no net import of Cl^- is expected under standard transport conditions (see Figure 8) even if the lumenal concentration of Cl^- is low. The notion that Cl^- is required for transporter activation but does not participate as a mandatory component in the transport cycle also helps explain why changes in cytoplasmic chloride do not appear to have drastic effects on the degree of vesicle filling. In the calyx of Held no change in quantal size was observed when dialyzed with varying chloride concentrations (Price and Trussell, 2006). These data suggest that external chloride binding solely affects uptake kinetics, but not the final amount of glutamate that can be loaded.

Although the model is capable of explaining most of the observed effects of chloride and potassium on vesicular glutamate uptake, there are still some loose ends. For instance, synaptic-like microvesicles isolated from astrocytes contain VGLUT1 and transport both glutamate and D-serine. Surprisingly, they do not show any chloride-dependent acidification, whereas glutamate causes acidification (Martineau et al., 2013). In contrast, in our experiments VGLUT alone is capable of mediating Cl^--dependent acidification which is partially competed for by high glutamate concentrations. Furthermore, the fact that VGLUT can function as a Na^+/phosphate cotransporter when exposed at the plasma membrane needs to be integrated into the emerging picture of the transporter, requiring further experiments. Juge and colleagues (Juge et al., 2006) have shown earlier that glutamate and phosphate transport appear to involve different sites, which would call for a third anion binding site that may, however, show overlap with one or both of the other two sites. Moreover, the role of Na^+ awaits further clarification: whereas we were unable to detect any effect of sodium on glutamate uptake in the reconstituted system, it is conceivable that in the presence of phosphate the cation binding site can also (or even preferentially) accommodate Na^+ ions.

Our model implies that VGLUT does not need other ion channels or transporters to fill a vesicle with glutamate. This notion is strongly supported by earlier work showing that VGLUT1 and VGLUT2, as well as VGLUT3, when transfected into GABAergic neurons, resulted in the release of glutamate with normal quantal size (Takamori et al., 2000, 2001; Weston et al., 2011). However, uptake is likely to be facilitated by other ion exchangers such as NHE6 or also ClC3 (or another relative), which support the maintenance of ionic and charge balance during transport. Interestingly, NHE7, which together with NHE6 and NHE9 was believed to exchange cytosolic K^+ with lumenal H^+ on intracellular compartments (Nakamura et al., 2005; Numata and Orlowski, 2001), has now been found to selectively transport Na^+ and Li^+, but not K^+ (Milosavljevic et al., 2014), in agreement with our finding that K^+ transport is mediated by VGLUT.

In summary, it is becoming apparent that VGLUTs share common mechanistic features with plasma membrane transporters of the solute carrier superfamily, such as EAATs and their bacterial orthologs. For instance, EAATs and its archebacterial ortholog GltPh display a conserved and nonstoichiometrically

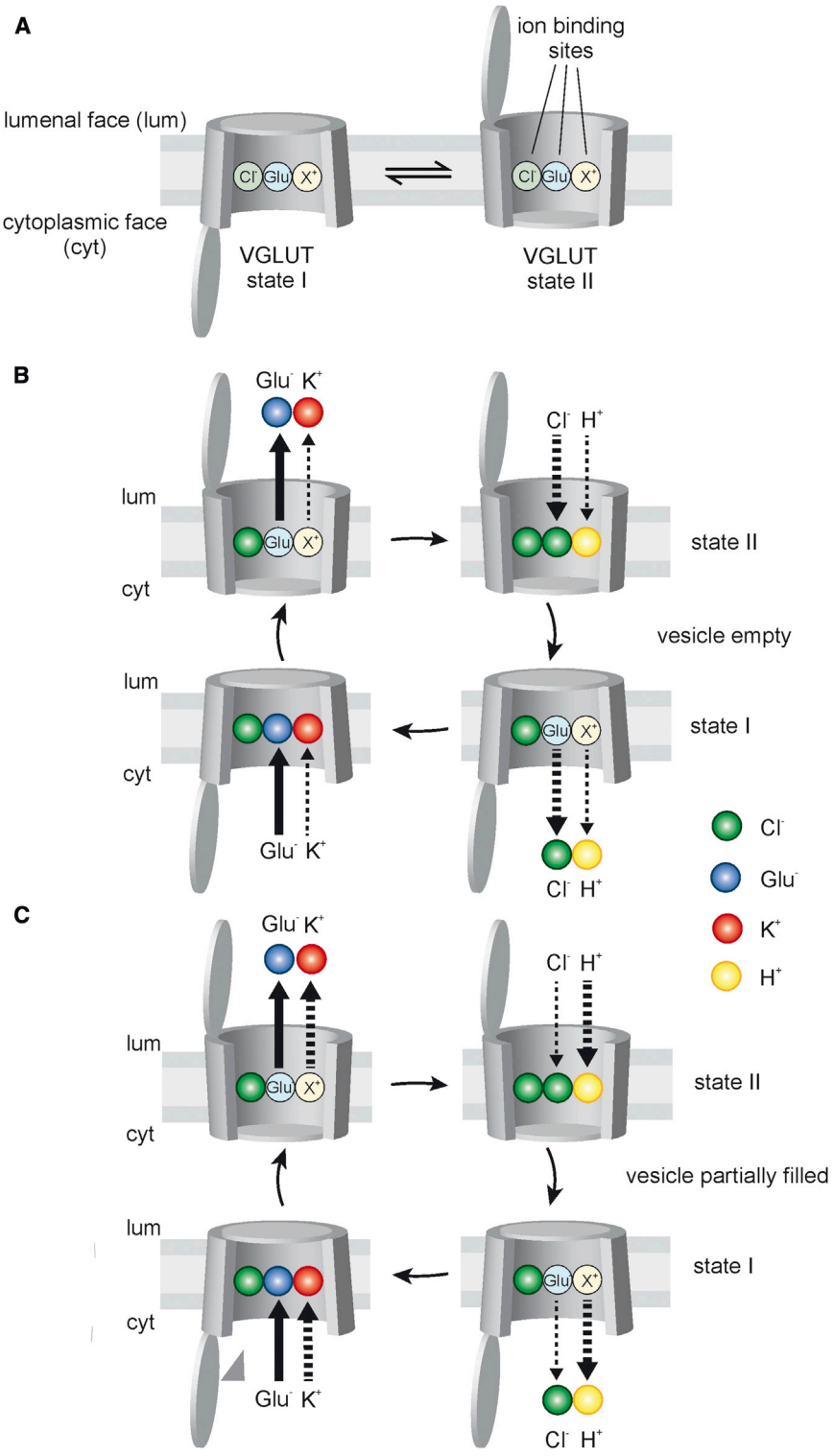

Figure 8. Model of Ion Transport Modes by VGLUT across the Vesicle Membrane
See text for details.

coupled chloride conductance (Ryan and Mindell, 2007; Vandenberg and Ryan, 2013), very similar to that described here. We expect that these similarities will become even more apparent in the future and may extend to other, less-well-characterized vesicular transporters.

EXPERIMENTAL PROCEDURES

Animals

Adult Wistar rats purchased from Charles River Laboratories, or Janvier S.A.S., and adult wild-type mice originated from the local animal house were kept until use at a 12:12 hr light/dark cycle with food and water ad libitum. ClC3 and VGLUT1 knockout mice were kindly provided by T.J. Jentsch (Leibniz-Institut für Molekulare Pharmakologie [FMP], 13125 Berlin, Germany) and C. Rosenmund (NeuroCure Cluster of Excellence, Charité, Universitätsmedizin Berlin, 10117 Berlin, Germany), respectively.

Antibodies

The following antibodies were purchased from Synaptic Systems (catalog numbers given in parentheses): mouse anti-VGLUT1 (135 311), anti-VGLUT2 (135 411), and anti-synaptophysin (101 011); rabbit anti-VGLUT1 (135 302), anti-VGLUT2 (135 402), anti-VGAT (131 002), and anti-synaptophysin (101 002). NHE6 goat polyclonal antibody was purchased from Santa Cruz Biotechnology, Inc.

Membrane Isolation

Synaptic vesicles (lysis pellet 2 [LP2] and SV fraction) were isolated according to previous publications from rat brain (Huttner et al., 1983; Nagy et al., 1976; Takamori et al., 2006). SVs were collected from the precleared supernatant after lysis by ultracentrifugation (LP2). This pellet is highly enriched in SVs and was used for neurotransmitter uptake (Zander et al., 2010) and hybrid SV formation without further purification. For the acridine orange experiments the LP2 fraction was further purified by sucrose density gradient centrifugation and size exclusion chromatography (SV fraction).

Membranes from PC12 cells expressing VGLUT2 were isolated by differential centrifugation following homogenization using a ball-bearing homogenizer (Barysch et al., 2010; Takamori et al., 2000). Immunoisolations were performed as described previously (Grønborg et al., 2010; Takamori et al., 2000; Zander et al., 2010). For details, see Supplemental Experimental Procedures.

Expression and Purification of Recombinant Proteins

VGLUT1 was expressed in insect cells using the baculovirus expression system (Hitchman et al., 2009; Luckow et al., 1993; Smith et al., 1983) and purified largely following a previously described protocol (Keefe et al., 2001; Schenck et al., 2009). For expression of the proton ATPase TF_oF_1, a plasmid carrying TF_oF_1 with a His_6-tagged β subunit (kindly provided by M. Yoshida [Suzuki et al., 2002]) was expressed in *E. coli* DK8 (Suzuki et al., 2002) and purified as given earlier (Schenck et al., 2009). A stabilized SNARE acceptor complex consisting of N-terminally truncated syntaxin-1A (aa

183–288), a C-terminal fragment of synaptobrevin 2 (49–96), and SNAP-25A expressed and purified as described (Pobbati et al., 2006; Stein et al., 2007). Detailed protocols are provided in the Supplemental Experimental Procedures.

Reconstitution of Proteins in Proteoliposomes and Generation of Hybrid Vesicles

Proteoliposomes were generated by detergent removal via dialysis from a mixture of the detergent-solubilized components (Rigaud and Lévy, 2003; Rigaud et al., 1995). The liposomes were composed of 1,2-dioleoyl-*sn*-glycero-3-phosphocholine (DOPC), 1,2-dioleoyl-*sn*-glycero-3-phospho-L-serine (DOPS) (both Avanti polar lipids) and cholesterol (Chol) at a molar ratio of DOPC:DOPS:Chol 65:10:25. The protein:lipid ratio (mol/mol) was adjusted to ~1:40,000 for TF_oF_1, to ~1:500 for the stabilized SNARE acceptor complex, and to ~1:2,000 for VGLUT1. For the generation of hybrid SVs, liposomes reconstituted with TF_oF_1 and the SNARE acceptor complex were fused with SVs for 45 min at room temperature as described (Holt et al., 2008). For details, see Supplemental Experimental Procedures.

Measurement of Glutamate Uptake, ΔpH, and ΔΨ

Glutamate uptake was performed as previously published (Hell et al., 1990; Maycox et al., 1988; Takamori et al., 2000). Acidification measurements were performed according to previous publications (Hell et al., 1990; Maycox et al., 1988) using acridine orange (AO, Molecular Probes) as a pH-sensitive dye (Palmgren, 1991). Measurements of changes in membrane potential were carried out using VGLUT1/TF_oF_1 liposomes and hybrid SVs using Oxonol VI (Molecular Probes), an anionic dye used to detect changes in ΔΨ (Hell et al., 1990; Russell, 1984; Shioi et al., 1989). For both acidification and potential measurements, the figures show representative traces. Note that baseline jumps occasionally observed upon addition of reagents were corrected (indicated by small gaps in the traces). Additional experimental details are available in the Supplemental Experimental Procedures.

SUPPLEMENTAL INFORMATION

Supplemental Information includes five figures and Supplemental Experimental Procedures and can be found with this article at http://dx.doi.org/10.1016/j.neuron.2014.11.008.

AUTHOR CONTRIBUTIONS

J.P. and J.-F.Z. carried out the experiments. T.S. provided the plasmid and critical input for the expression and purification of the TF_oF_1-ATPase required for reconstitution. G.A.-H. and R.J. coordinated the work. All authors were involved in preparation and finalization of the manuscript.

ACKNOWLEDGMENTS

We would like to thank Ursel Ries and Gottfried Mieskes for valuable technical assistance, and Matías Hernández, Stephan Schenck, Geert van den Boogart, and Zohreh Farsi for helpful discussions. This work was supported by a grant from the Deutsche Forschungsgemeinschaft to G.A.-H. and R.J.

Accepted: November 4, 2014
Published: November 26, 2014

REFERENCES

Ahnert-Hilger, G., Höltje, M., Pahner, I., Winter, S., and Brunk, I. (2003). Regulation of vesicular neurotransmitter transporters. Rev. Physiol. Biochem. Pharmacol. *150*, 140–160.

Aihara, Y., Mashima, H., Onda, H., Hisano, S., Kasuya, H., Hori, T., Yamada, S., Tomura, H., Yamada, Y., Inoue, I., et al. (2000). Molecular cloning of a novel brain-type Na(+)-dependent inorganic phosphate cotransporter. J. Neurochem. *74*, 2622–2625.

Alpern, R.J., Cogan, M.G., and Rector, F.C., Jr. (1983). Effects of extracellular fluid volume and plasma bicarbonate concentration on proximal acidification in the rat. J. Clin. Invest. *71*, 736–746.

Barysch, S.V., Jahn, R., and Rizzoli, S.O. (2010). A fluorescence-based *in vitro* assay for investigating early endosome dynamics. Nat. Protoc. *5*, 1127–1137.

Bellocchio, E.E., Reimer, R.J., Fremeau, R.T., Jr., and Edwards, R.H. (2000). Uptake of glutamate into synaptic vesicles by an inorganic phosphate transporter. Science *289*, 957–960.

Biwersi, J., Tulk, B., and Verkman, A.S. (1994). Long-wavelength chloride-sensitive fluorescent indicators. Anal. Biochem. *219*, 139–143.

Danbolt, N.C. (2001). Glutamate uptake. Prog. Neurobiol. *65*, 1–105.

Deitmer, J.W., and Rose, C.R. (1996). pH regulation and proton signalling by glial cells. Prog. Neurobiol. *48*, 73–103.

Edwards, R.H. (2007). The neurotransmitter cycle and quantal size. Neuron *55*, 835–858.

El Mestikawy, S., Wallén-Mackenzie, A., Fortin, G.M., Descarries, L., and Trudeau, L.E. (2011). From glutamate co-release to vesicular synergy: vesicular glutamate transporters. Nat. Rev. Neurosci. *12*, 204–216.

Focke, P.J., Wang, X., and Larsson, H.P. (2013). Neurotransmitter transporters: structure meets function. Structure *21*, 694–705.

Füldner, H.H., and Stadler, H. (1982). ^{31}P-NMR analysis of synaptic vesicles. Status of ATP and internal pH. Eur. J. Biochem. *121*, 519–524.

Goh, G.Y., Huang, H., Ullman, J., Borre, L., Hnasko, T.S., Trussell, L.O., and Edwards, R.H. (2011). Presynaptic regulation of quantal size: K^+/H^+ exchange stimulates vesicular glutamate transport. Nat. Neurosci. *14*, 1285–1292.

Goldsmith, D.J., and Hilton, P.J. (1992). Relationship between intracellular proton buffering capacity and intracellular pH. Kidney Int. *41*, 43–49.

Gouaux, E. (2009). Review. The molecular logic of sodium-coupled neurotransmitter transporters. Philos. Trans. R. Soc. Lond. B Biol. Sci. *364*, 149–154.

Grønborg, M., Pavlos, N.J., Brunk, I., Chua, J.J., Münster-Wandowski, A., Riedel, D., Ahnert-Hilger, G., Urlaub, H., and Jahn, R. (2010). Quantitative comparison of glutamatergic and GABAergic synaptic vesicles unveils selectivity for few proteins including MAL2, a novel synaptic vesicle protein. J. Neurosci. *30*, 2–12.

Hartinger, J., and Jahn, R. (1993). An anion binding site that regulates the glutamate transporter of synaptic vesicles. J. Biol. Chem. *268*, 23122–23127.

Hell, J.W., Maycox, P.R., and Jahn, R. (1990). Energy dependence and functional reconstitution of the gamma-aminobutyric acid carrier from synaptic vesicles. J. Biol. Chem. *265*, 2111–2117.

Henderson, P.J. (1971). Ion transport by energy-conserving biological membranes. Annu. Rev. Microbiol. *25*, 393–428.

Hernandez, J.M., Stein, A., Behrmann, E., Riedel, D., Cypionka, A., Farsi, Z., Walla, P.J., Raunser, S., and Jahn, R. (2012). Membrane fusion intermediates via directional and full assembly of the SNARE complex. Science *336*, 1581–1584.

Hitchman, R.B., Possee, R.D., and King, L.A. (2009). Baculovirus expression systems for recombinant protein production in insect cells. Recent Pat. Biotechnol. *3*, 46–54.

Holt, M., Riedel, D., Stein, A., Schuette, C., and Jahn, R. (2008). Synaptic vesicles are constitutively active fusion machines that function independently of Ca^{2+}. Curr. Biol. *18*, 715–722.

Huttner, W.B., Schiebler, W., Greengard, P., and De Camilli, P. (1983). Synapsin I (protein I), a nerve terminal-specific phosphoprotein. III. Its association with synaptic vesicles studied in a highly purified synaptic vesicle preparation. J. Cell Biol. *96*, 1374–1388.

Jentsch, T.J., Friedrich, T., Schriever, A., and Yamada, H. (1999). The CLC chloride channel family. Pflugers Arch. *437*, 783–795.

Johnson, R.G., Jr. (1988). Accumulation of biological amines into chromaffin granules: a model for hormone and neurotransmitter transport. Physiol. Rev. *68*, 232–307.

Juge, N., Yoshida, Y., Yatsushiro, S., Omote, H., and Moriyama, Y. (2006). Vesicular glutamate transporter contains two independent transport machineries. J. Biol. Chem. *281*, 39499–39506.

Juge, N., Gray, J.A., Omote, H., Miyaji, T., Inoue, T., Hara, C., Uneyama, H., Edwards, R.H., Nicoll, R.A., and Moriyama, Y. (2010). Metabolic control of vesicular glutamate transport and release. Neuron *68*, 99–112.

Keefe, A.D., Wilson, D.S., Seelig, B., and Szostak, J.W. (2001). One-step purification of recombinant proteins using a nanomolar-affinity streptavidin-binding peptide, the SBP-Tag. Protein Expr. Purif. *23*, 440–446.

Krishnamurthy, H., Piscitelli, C.L., and Gouaux, E. (2009). Unlocking the molecular secrets of sodium-coupled transporters. Nature *459*, 347–355.

Luckow, V.A., Lee, S.C., Barry, G.F., and Olins, P.O. (1993). Efficient generation of infectious recombinant baculoviruses by site-specific transposon-mediated insertion of foreign genes into a baculovirus genome propagated in Escherichia coli. J. Virol. *67*, 4566–4579.

Martineau, M., Shi, T., Puyal, J., Knolhoff, A.M., Dulong, J., Gasnier, B., Klingauf, J., Sweedler, J.V., Jahn, R., and Mothet, J.P. (2013). Storage and uptake of D-serine into astrocytic synaptic-like vesicles specify gliotransmission. J. Neurosci. *33*, 3413–3423.

Maycox, P.R., Deckwerth, T., Hell, J.W., and Jahn, R. (1988). Glutamate uptake by brain synaptic vesicles. Energy dependence of transport and functional reconstitution in proteoliposomes. J. Biol. Chem. *263*, 15423–15428.

Maycox, P.R., Hell, J.W., and Jahn, R. (1990). Amino acid neurotransmission: spotlight on synaptic vesicles. Trends Neurosci. *13*, 83–87.

Michaelson, D.M., and Angel, I. (1980). Determination of delta pH in cholinergic synaptic vesicles: its effect on storage and release of acetylcholine. Life Sci. *27*, 39–44.

Milosavljevic, N., Monet, M., Léna, I., Brau, F., Lacas-Gervais, S., Feliciangeli, S., Counillon, L., and Poët, M. (2014). The intracellular $Na(^{+})/H(^{+})$ exchanger NHE7 effects a $Na(^{+})$-coupled, but not $K(^{+})$-coupled proton-loading mechanism in endocytosis. Cell Rep. *7*, 689–696.

Muench, S.P., Trinick, J., and Harrison, M.A. (2011). Structural divergence of the rotary ATPases. Q. Rev. Biophys. *44*, 311–356.

Nagy, A., Baker, R.R., Morris, S.J., and Whittaker, V.P. (1976). The preparation and characterization of synaptic vesicles of high purity. Brain Res. *109*, 285–309.

Naito, S., and Ueda, T. (1985). Characterization of glutamate uptake into synaptic vesicles. J. Neurochem. *44*, 99–109.

Nakamura, N., Tanaka, S., Teko, Y., Mitsui, K., and Kanazawa, H. (2005). Four Na^{+}/H^{+} exchanger isoforms are distributed to Golgi and post-Golgi compartments and are involved in organelle pH regulation. J. Biol. Chem. *280*, 1561–1572.

Nguyen, M.L., and Parsons, S.M. (1995). Effects of internal pH on the acetylcholine transporter of synaptic vesicles. J. Neurochem. *64*, 1137–1142.

Nguyen, M.L., Cox, G.D., and Parsons, S.M. (1998). Kinetic parameters for the vesicular acetylcholine transporter: two protons are exchanged for one acetylcholine. Biochemistry *37*, 13400–13410.

Ni, B., Rosteck, P.R., Jr., Nadi, N.S., and Paul, S.M. (1994). Cloning and expression of a cDNA encoding a brain-specific Na(+)-dependent inorganic phosphate cotransporter. Proc. Natl. Acad. Sci. USA *91*, 5607–5611.

Numata, M., and Orlowski, J. (2001). Molecular cloning and characterization of a novel $(Na^{+},K^{+})/H^{+}$ exchanger localized to the *trans*-Golgi network. J. Biol. Chem. *276*, 17387–17394.

Omote, H., and Moriyama, Y. (2013). Vesicular neurotransmitter transporters: an approach for studying transporters with purified proteins. Physiology (Bethesda) *28*, 39–50.

Palmgren, M.G. (1991). Acridine orange as a probe for measuring pH gradients across membranes: mechanism and limitations. Anal. Biochem. *192*, 316–321.

Pobbati, A.V., Stein, A., and Fasshauer, D. (2006). N- to C-terminal SNARE complex assembly promotes rapid membrane fusion. Science *313*, 673–676.

Price, G.D., and Trussell, L.O. (2006). Estimate of the chloride concentration in a central glutamatergic terminal: a gramicidin perforated-patch study on the calyx of Held. J. Neurosci. *26*, 11432–11436.

Reigada, D., Díez-Pérez, I., Gorostiza, P., Verdaguer, A., Gómez de Aranda, I., Pineda, O., Vilarrasa, J., Marsal, J., Blasi, J., Aleu, J., and Solsona, C. (2003). Control of neurotransmitter release by an internal gel matrix in synaptic vesicles. Proc. Natl. Acad. Sci. USA *100*, 3485–3490.

Rigaud, J.L., and Lévy, D. (2003). Reconstitution of membrane proteins into liposomes. Methods Enzymol. *372*, 65–86.

Rigaud, J.L., Pitard, B., and Levy, D. (1995). Reconstitution of membrane proteins into liposomes: application to energy-transducing membrane proteins. Biochim. Biophys. Acta *1231*, 223–246.

Rudnick, G. (2011). Cytoplasmic permeation pathway of neurotransmitter transporters. Biochemistry *50*, 7462–7475.

Russell, J.T. (1984). Δ pH, H^{+} diffusion potentials, and Mg^{2+} ATPase in neurosecretory vesicles isolated from bovine neurohypophyses. J. Biol. Chem. *259*, 9496–9507.

Ryan, R.M., and Mindell, J.A. (2007). The uncoupled chloride conductance of a bacterial glutamate transporter homolog. Nat. Struct. Mol. Biol. *14*, 365–371.

Schenck, S., Wojcik, S.M., Brose, N., and Takamori, S. (2009). A chloride conductance in VGLUT1 underlies maximal glutamate loading into synaptic vesicles. Nat. Neurosci. *12*, 156–162.

Shioi, J., Naito, S., and Ueda, T. (1989). Glutamate uptake into synaptic vesicles of bovine cerebral cortex and electrochemical potential difference of proton across the membrane. Biochem. J. *258*, 499–504.

Smith, G.E., Fraser, M.J., and Summers, M.D. (1983). Molecular engineering of the *Autographa californica* nuclear polyhedrosis virus genome: deletion mutations within the polyhedrin gene. J. Virol. *46*, 584–593.

Stein, A., Radhakrishnan, A., Riedel, D., Fasshauer, D., and Jahn, R. (2007). Synaptotagmin activates membrane fusion through a Ca^{2+}-dependent *trans* interaction with phospholipids. Nat. Struct. Mol. Biol. *14*, 904–911.

Stobrawa, S.M., Breiderhoff, T., Takamori, S., Engel, D., Schweizer, M., Zdebik, A.A., Bösl, M.R., Ruether, K., Jahn, H., Draguhn, A., et al. (2001). Disruption of ClC-3, a chloride channel expressed on synaptic vesicles, leads to a loss of the hippocampus. Neuron *29*, 185–196.

Suzuki, T., Ueno, H., Mitome, N., Suzuki, J., and Yoshida, M. (2002). F(0) of ATP synthase is a rotary proton channel. Obligatory coupling of proton translocation with rotation of c-subunit ring. J. Biol. Chem. *277*, 13281–13285.

Tabb, J.S., Kish, P.E., Van Dyke, R., and Ueda, T. (1992). Glutamate transport into synaptic vesicles. Roles of membrane potential, pH gradient, and intravesicular pH. J. Biol. Chem. *267*, 15412–15418.

Takamori, S., Rhee, J.S., Rosenmund, C., and Jahn, R. (2000). Identification of a vesicular glutamate transporter that defines a glutamatergic phenotype in neurons. Nature *407*, 189–194.

Takamori, S., Rhee, J.S., Rosenmund, C., and Jahn, R. (2001). Identification of differentiation-associated brain-specific phosphate transporter as a second vesicular glutamate transporter (VGLUT2). J. Neurosci. *21*, RC182.

Takamori, S., Holt, M., Stenius, K., Lemke, E.A., Grønborg, M., Riedel, D., Urlaub, H., Schenck, S., Brügger, B., Ringler, P., et al. (2006). Molecular anatomy of a trafficking organelle. Cell *127*, 831–846.

Toei, M., Saum, R., and Forgac, M. (2010). Regulation and isoform function of the V-ATPases. Biochemistry *49*, 4715–4723.

van den Bogaart, G., Holt, M.G., Bunt, G., Riedel, D., Wouters, F.S., and Jahn, R. (2010). One SNARE complex is sufficient for membrane fusion. Nat. Struct. Mol. Biol. *17*, 358–364.

Vandenberg, R.J., and Ryan, R.M. (2013). Mechanisms of glutamate transport. Physiol. Rev. *93*, 1621–1657.

Verkman, A.S. (1990). Development and biological applications of chloride-sensitive fluorescent indicators. Am. J. Physiol. *259*, C375–C388.

Weston, M.C., Nehring, R.B., Wojcik, S.M., and Rosenmund, C. (2011). Interplay between VGLUT isoforms and endophilin A1 regulates neurotransmitter release and short-term plasticity. Neuron *69*, 1147–1159.

Winter, S., Brunk, I., Walther, D.J., Höltje, M., Jiang, M., Peter, J.U., Takamori, S., Jahn, R., Birnbaumer, L., and Ahnert-Hilger, G. (2005). Galphao2 regulates vesicular glutamate transporter activity by changing its chloride dependence. J. Neurosci. *25*, 4672–4680.

Wolosker, H., de Souza, D.O., and de Meis, L. (1996). Regulation of glutamate transport into synaptic vesicles by chloride and proton gradient. J. Biol. Chem. *271*, 11726–11731.

Xie, X.S., Stone, D.K., and Racker, E. (1983). Determinants of clathrin-coated vesicle acidification. J. Biol. Chem. *258*, 14834–14838.

Zander, J.F., Münster-Wandowski, A., Brunk, I., Pahner, I., Gómez-Lira, G., Heinemann, U., Gutiérrez, R., Laube, G., and Ahnert-Hilger, G. (2010). Synaptic and vesicular coexistence of VGLUT and VGAT in selected excitatory and inhibitory synapses. J. Neurosci. *30*, 7634–7645.

Neuron, Volume *84*

Supplemental Information

Vesicular Glutamate Transporters Use Flexible Anion and Cation Binding Sites for Efficient Accumulation of Neurotransmitter

Julia Preobraschenski, Johannes-Friedrich Zander, Toshiharu Suzuki, Gudrun Ahnert-Hilger, and Reinhard Jahn

SUPPLEMENTAL INFORMATION

SUPPLEMENTAL FIGURES

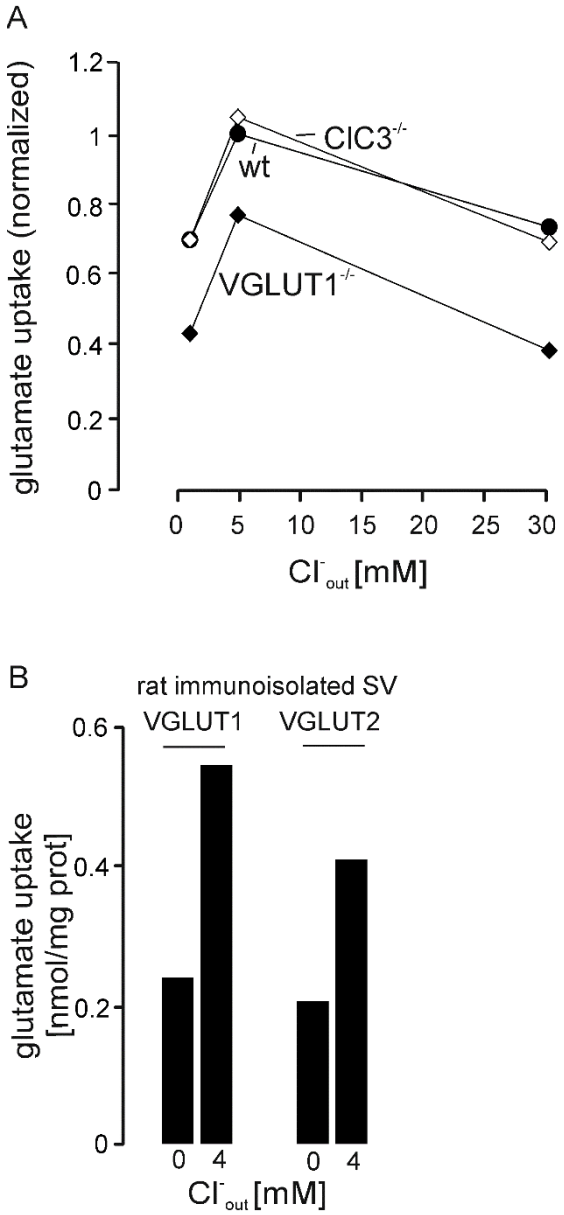

Figure S1: Cl^- dependence of VGLUT-mediated glutamate uptake is independent of the isoform and does not require the Cl^- channel ClC3, related to Figure 1. A: Cl^-- dependence of glutamate uptake by SV isolated from wild type, $VGLUT1^{-/-}$, or $ClC3^{-/-}$ mice. Data represent FCCP-sensitive uptake and are normalized to uptake at 4 mM chloride of the respective wild type.* B: Glutamate uptake by SV immunoisolated from rat brain using antibodies specific for VGLUT 1 or 2, respectively. The immunoisolated vesicles are highly enriched for their respective antigens, with only very limited overlap (Zander et al., 2010). Values are expressed as nmol/mg protein.* (*n=1).

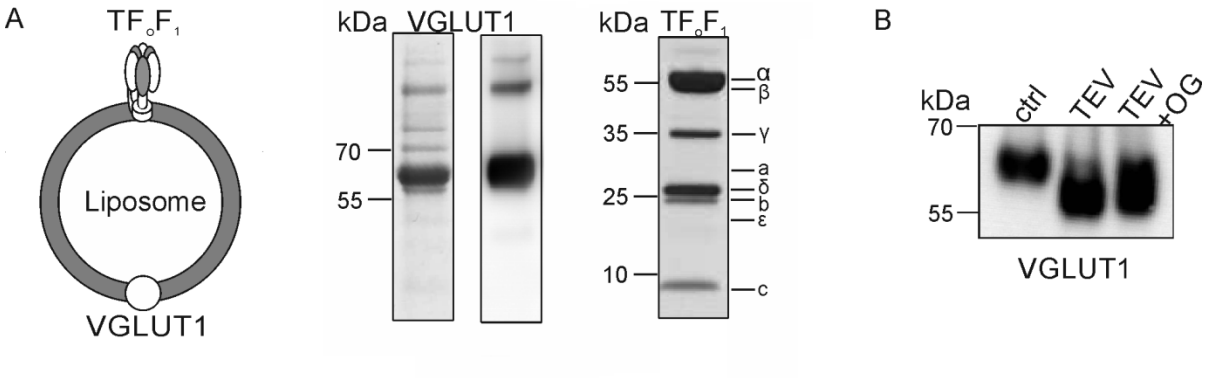

Figure S2: Characterization of proteoliposomes containing purified recombinant VGLUT1 and the proton ATPase TF_oF_1, related to Figure 2. A: Coomassie Blue-stained SDS-polyacrylamide gels (10%) of the purified proteins (5µg protein/lane) and an immunoblot for VGLUT1 (1µg). B: After reconstitution, VGLUT1 is predominantly oriented with the cytoplasmic side facing outward. VGLUT1 containing an N-terminal streptavidin binding peptide tag was reconstituted in liposomes and incubated with TEV protease (TEV) in the absence or presence of the detergent n-Octyl-β-D-glucopyranoside (OG) (TEV+OG). Note that an almost quantitative shift is observed under both conditions.

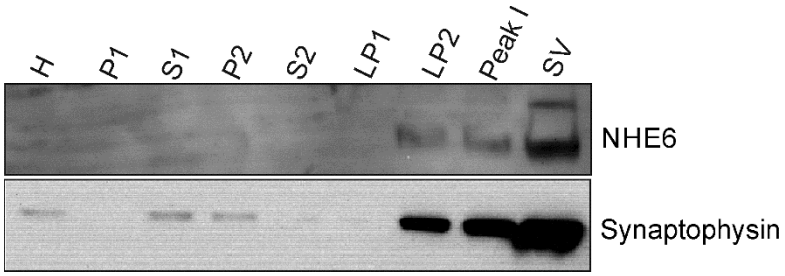

Figure S3: The cation/proton exchanger NHE6 co-purifies with synaptic vesicles, related to Figure 4. Synaptic vesicles were purified from rat brain homogenate (H) using a standard protocol involving the isolation of synaptosomes (P2), followed by lysis of synaptosomes and stepwise enrichment of SVs using differential centrifugation (LP2) sucrose density gradient centrifugation, and size-exclusion chromatography on controlled-pore glass beads (Huttner et al., 1983). Two peaks elute from the column, with peak I containing mainly contaminating membranes and peak II (SV) containing synaptic vesicles at over 90% purity. Equal amounts of protein (20µg/fraction) were analyzed by immunoblotting for NHE6 and the synaptic vesicle marker synaptophysin. Both proteins are highly enriched in the purified SV fraction.

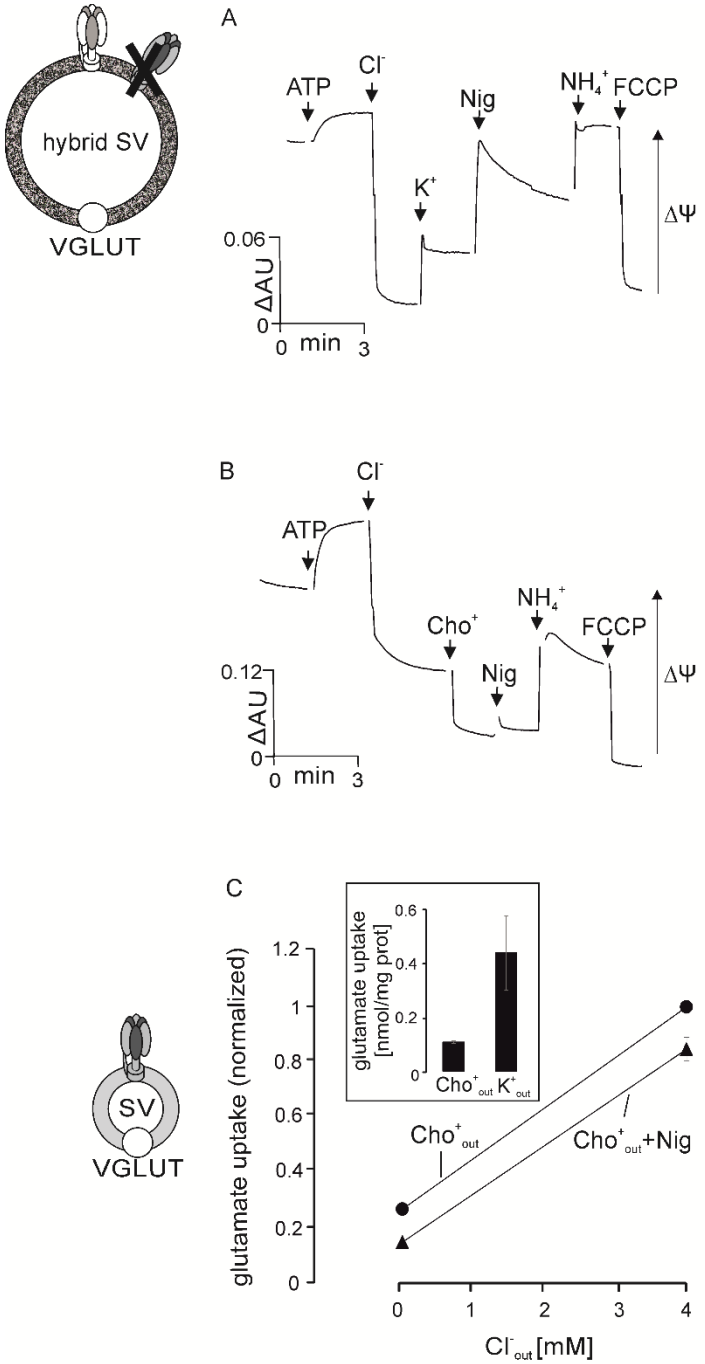

Figure S4: K^+ enhances glutamate uptake by increasing ΔΨ in hybrid vesicles by H^+ exchange, related to Figure 5. A: Changes in ΔΨ, measured with the dye Oxonol VI, in hybrid vesicles preloaded with 150 mM choline gluconate in 300 mM external glycine buffer. The additions were ATP, 30 mM choline chloride (Cl^-) and K-gluconate (K^+), 5 nM nigericin (Nig), 5 mM $(NH_4)_2SO_4$ (NH_4^+) and FCCP. Addition of ATP results in proton pumping causing an increase in ΔΨ. Addition of Cl^- results in Cl^- import, neutralizing the positive charges (net import of HCl), resulting in a drop of ΔΨ. Subsequent addition of K^+ results in proton export, increasing proton pumping and thus resulting in an increase of in ΔΨ that is further enhanced by the Nig that operates as K^+/H^+ exchanger under these conditions. NH_4^+ abolishes the pH-gradient and thus increases ΔΨ. FCCP dissipates both components of the electrochemical potential. Arrows are indicative of the substrate addition time points. B: Same as in A, but K^+ was replaced with the impermeant cation choline (Cho^+). Neither Cho^+ nor nigericin increased ΔΨ as expected. C: Glutamate uptake by synaptic vesicles (LP2 fraction) at 0 and 4 mM choline chloride was performed at 150mM external choline gluconate and with (Cho^+_{out}+Nig) and without 50 nM nigericin (Cho^+_{out}). Note that nigericin did not stimulate glutamate uptake in absence of K^+. The inset shows glutamate uptake at 4 mM Cl^- in presence of K-gluconate (K^+_{out}) and choline gluconate (Cho^+_{out}). Mean values with bars representing the experimental range. n=1-2.

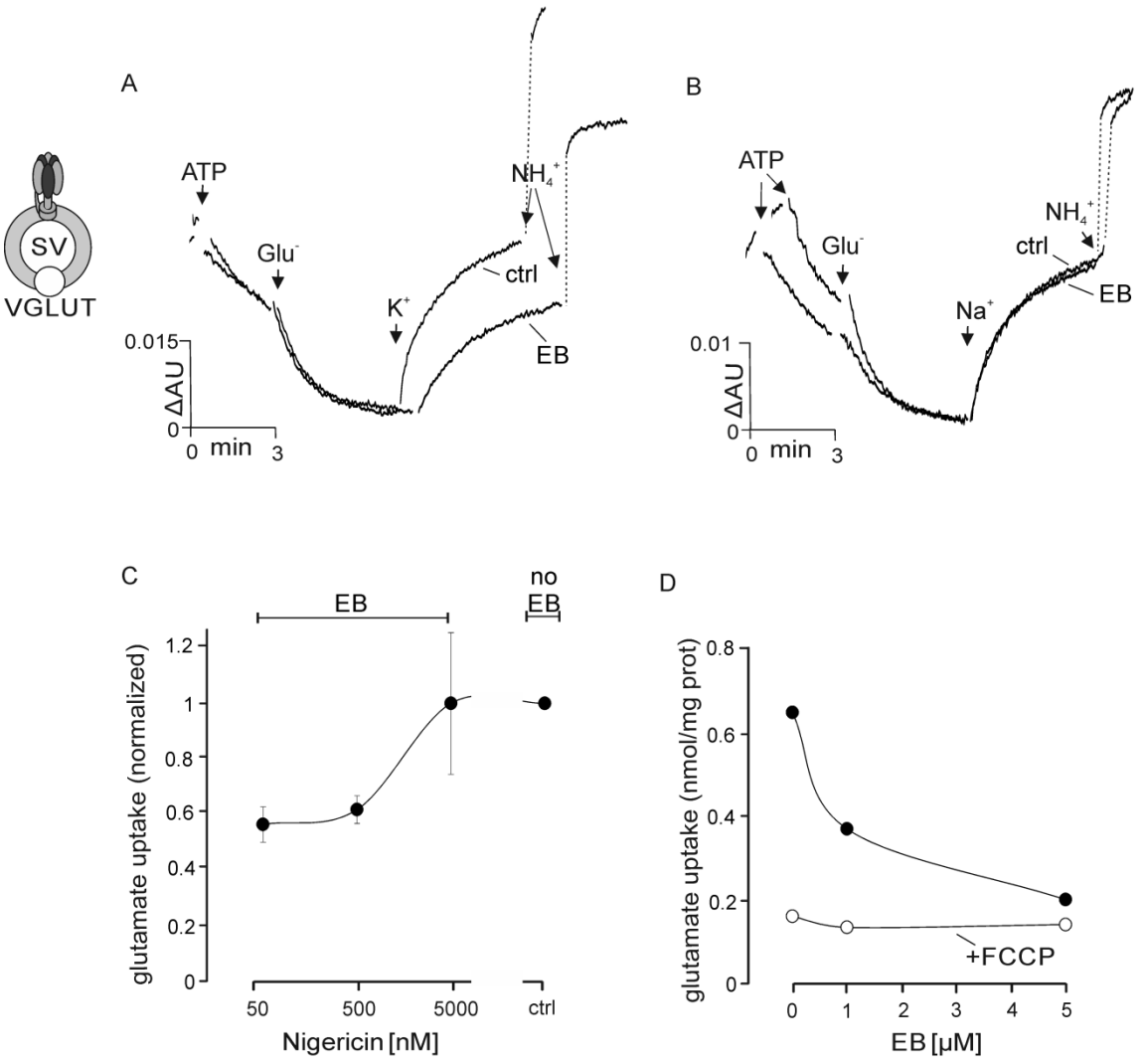

Figure S5: Evans Blue inhibits glutamate by binding to the cation binding site of VGLUT, related to Figure 6. A, B: Glutamate induced acidification of SVs (SV-fraction) is not affected by Evans Blue (EB, 1.5 µM) but reversal by K^+ (A) but not by Na^+ (B) is inhibited (see figure 2 for details of the assay). The additions were ATP (1.2 mM) to start the reaction, choline glutamate (Glu^-) (10 mM), which induces acidification, K^+ and Na^+ (added at 30 mM as gluconate salts), and finally 20 mM $(NH_4)_2SO_4$ (NH_4^+) to disperse ΔpH. Note that EB partially blocks reversal of ΔpH by K^+ but not by Na^+, in agreement with the selective stimulation of glutamate uptake by K^+. A dual wavelength spectrophotometer was used which enables detection of changes in acridine orange absorbance despite a high background absorbance caused by the presence of EB. C: Nigericin reverses inhibition of glutamate uptake by Evans Blue (1µM) in a dose-dependent manner. In the assay, synaptic vesicles (LP2-fraction) were used. Data were normalized to the value obtained in the absence of inhibitor and represent mean values of n=2 with bars indicating the experimental range. D: Glutamate uptake by synaptic vesicles (LP2-fraction) at varying concentrations of Evans Blue (EB) in the absence and presence of the proton ionophore FCCP shows that Evans Blue does not completely inhibit proton-gradient dependent glutamate uptake (data from a single experiment).

SUPPLEMENTAL EXPERIMENTAL PROCEDURES

Immunoisolation

Immunoisolations of synaptic vesicles were performed according to previously published protocols (Gronborg et al., 2010; Takamori et al., 2000; Zander et al., 2010). In brief, paramagnetic beads (Dynabeads Pan Mouse IgG, Life Technologies) containing covalently linked antibodies specific for all mouse IgG subclasses were first incubated with the respective primary mouse antibodies (Synaptic Systems) suspended in coating buffer [PBS, pH 7.4, 0.1% BSA (w/v)]. Affinity-purified mouse antibodies were supplied at a concentration of 0.5 – 1 µg of IgG per 10^7 beads and rotated for 2 h at 4°C. The coated beads were washed four times in coating buffer. Immunoisolation was performed overnight at 4°C under rotation using a suspension of the coated beads and an LS1 fraction diluted with incubation buffer [PBS, pH 7.4, 2 mM EDTA, and 5% BSA (w/v)] to yield a ratio of 75 µg protein to 1.4 x10^7 beads. The beads were washed three times in incubation buffer, and three times in coating buffer. Beads without primary antibodies were subjected to the same procedures and served as control for non-specifically bound material (Zander et al., 2010).

Preparation of light membrane fractions from PC12 cells

VGLUT2-PC12 and mock-PC12 cells (kindly provided by Lutz Birnbaumer, Department of Neurobiology,Division of Intramural Research, National Institute of Environmental Health Sciences, Research Triangle Park, North Carolina USA) were grown (DMEM, 5 % FCS, 10 % HS, 2 mM L-glutamate and PenStrep, 37 °C, 10 % CO_2) to a confluency of ~60 %. Cells of five 10 cm dishes were resuspended in 1 ml sucrose buffer (320 mM sucrose, 10 mM MOPS-Tris, pH 7.3, 2 mM $MgSO_4$) and homogenized using a ball-bearing homogenizer (10 µm clearance) (Barysch et al., 2010; Takamori et al., 2000). To remove debris and larger particles including mitochondria, the homogenate was centrifuged for 10 min at 10,000xg. The resulting supernatant containing the light membranes was submitted to ultracentrifugation at 200,000xg for 20 min (S140AT rotor, Sorvall). The resulting membrane pellet was resuspended in ~ 100-150 µl sucrose buffer.

Expression and purification of recombinant proteins

VGLUT1: VGLUT1 was expressed in insect cells using the baculovirus expression system (Hitchman et al., 2009; Luckow et al., 1993; Smith et al., 1983). Streptavidin binding peptide (SBP)-tagged (Keefe et al., 2001; Schenck et al., 2009) *mus musculus* VGLUT1 cDNA (in pDEST8 vector, Gateway® baculovirus vector, Invitrogen) was inserted into the bacmid EMBacY (baculovirus coding DNA with an integrated yellow fluorescent protein (YFP) expression marker) via Tn7 transposition in DH10 bacterial strain (Bieniossek et al., 2008; Luckow et al., 1993). The VGLUT1 cDNA carrying bacmid was transfected in *Spodoptera frugiperda* cells (Sf9, in Sf900 media, Invitrogen) and cultured at 27 °C in suspension culture until a sufficient viral titer was obtained. *Trichoplusia ni* (High5, Invitrogen) cells in suspension culture (0.7 * 10^6 cells/ml, Express Five media, Invitrogen) were used for protein expression. VGLUT1 expression was monitored by measurement of YFP fluorescence and was maximal 36 h post-infection with 10 mg/l protein expressed. High5 cells were harvested 36-48 h post-infection and processed for VGLUT1 isolation.

The VGLUT1 purification procedure followed a protocol given earlier with some modifications (Schenck et al., 2009). Briefly, High5 cells from 1 l culture were resuspended in 50 ml of ice cold

resuspension buffer (40 mM Tris, pH 7.3, 300 mM KCl, 2 mM EDTA) with 1 x Protease Inhibitor Cocktail (EDTA free, Merck) and 5 mM β-mercaptoethanol. N-dodecyl-β-D-maltopyranoside (DDM, Glycon) was added to a final concentration of 2 % (w/v) and cells were lysed for 1 h at 4 °C under constant rotation. Subsequently, cell debris were removed by centrifugation at 250,000 xg (70Ti rotor, Beckman Coulter) for 20 min at 4 °C. The supernatant was supplemented with 1 ml streptavidin beads (Pierce) and rotated for 3 h at 4 °C. The beads were washed with 2 x 10 resin volumes of wash buffer (resuspension buffer containing 0.1 % DDM) and the protein was finally eluted with 5 x 1 resin volume of elution buffer (15 mM Tris, pH 7.3, 100 mM KCl, 0.6 mM EDTA, 2 mM (+) biotin, 5 mM β-mercaptoethanol and 0.05 % DDM). The beads were incubated for 5 min on ice for each elution step. The elution fractions were pooled and concentrated using a 30 kDa MWCO VivaSpin concentrator (Sartorius) to yield a final protein concentration of ~1 mg/ml (~ 3-5 fold). Due to its large micelle size (~50 kDa) DDM accumulated in the concentrated protein sample to a final concentration of ~0.25 %. Concentrated VGLUT1 was snap frozen in aliquots and stored at -80 °C. 1 l of High5 expression culture yielded ~ 0.7 mg of purified VGLUT protein.

Proton ATPase TF_oF_1: The pTR19-ASDS plasmid carrying TF_oF_1 with a His_6-tagged β-subunit was kindly provided by M. Yoshida (Suzuki et al., 2002). TF_oF_1 was expressed in *E.coli* DK8 (Suzuki et al., 2002) and purified as given earlier (Schenck et al., 2009) with slight modifications. The affinity purification with Talon beads (Clontech) was performed at 4 °C followed by anion exchange chromatography at room temperature using the ÄKTA system (GE Healthcare). The protein was supplemented with 10% glycerol, snap frozen and stored at -80 °C.

SNARE proteins: The ΔN complex constructs consist of the pETDuet-1 vector carrying syntaxin-1A (183-288) and the C-terminal fragment of synaptobrevin 2 (49-96) and the pET28a vector carrying His_6-tagged SNAP-25A (Pobbati et al., 2006; Stein et al., 2007). All cDNAs originated from *Rattus norvegicus* and were used for co-expression. The components of the ΔN complex, syntaxin-1A (183-288), synaptobrevin 2 (49-96) and SNAP-25A were co-expressed in *E.coli* BL21(DE3) and purified as previously described (Pobbati et al., 2006; Stein et al., 2007). Ni^{2+}-NTA affinity purification was followed by anion exchange chromatography using the ÄKTA system (GE Healthcare).

Preparation of proteoliposomes

Proteoliposomes were generated by detergent removal via dialysis from a mixture of the detergent-solubilised components (Rigaud and Levy, 2003; Rigaud et al., 1995). In detail, the synthetic lipid mix consisting of 1,2-dioleoyl-*sn*-glycero-3-phosphocholine (DOPC), 1,2-dioleoyl-*sn*-glycero-3-phospho-L-serine (DOPS) (both Avanti Polar Lipids) and Cholesterol (Chol) (from sheep wool, Avanti Polar Lipids) at a molar ratio of DOPC:DOPS:Chol 65:10:25 was formed by evaporating the organic solvent from the lipids and dissolving the dried lipid film in buffer (300 mM Glycine, 10 mM MOPS-Tris, pH 7.3, 2 mM $MgSO_4$, 5% n-Octyl-β-D-glucopyranosid) to a concentration of 10mg/ml lipids. The protein:lipid ratio (mol/mol) was adjusted to ~1:40000 for TF_oF_1, to ~1:500 for the ΔN complex and to ~1:2000 for VGLUT1. The final lipid concentration was adjusted to 3.6 mM. After mixing, the respective solutions were dialysed in Slide-A-Lyzer dialysis cassettes (2 kDa MWCO, Thermo Scientific) over night at 4 °C in 300 mM glycine, 150 mM choline gluconate or choline chloride, 10 mM MOPS-Tris, pH 7.3, and 2 mM $MgSO_4$ if not otherwise indicated. The dialysis buffer was additionally supplemented with 2 g BioBeads (BioRad) to adsorb detergent monomers. After dialysis, remaining

DDM in the VGLUT1/TF_oF_1 liposomes was complexed with 2,6-di-O-methyl-β-cyclodextrin (β-CD, Sigma) (Degrip et al., 1998; Schenck et al., 2009) by adding a few crumbs of solid β-CD to the liposomes and incubating them on ice for 1 h by occasionally inverting the tubes. External buffer exchange was performed by size exclusion chromatography (PD10, GE Healthcare). Up to 1 ml of liposome suspension was applied to one column. The liposome fractions were identified by their viscous and turbid appearance and collected separately. The samples were diluted 1.5-2 fold. The size distribution of the formed liposomes was measured using Dynamic Light Scattering.

Generation of hybrid SVs

TF_oF_1/ΔN liposomes were fused with SVs for 45 min at room temperature (Holt et al., 2008). Per data point, typically 30 µg of LP2 were mixed with 12 µl of liposomes and adjusted to 50 µl with reconstitution buffer (150 mM choline gluconate or choline chloride, 10 mM MOPS, 2 mM $MgSO_4$, pH 7.3). For external buffer exchange the samples were loaded on pre-packed size exclusion columns (PD10, GE Healthcare) (see proteoliposomes). The dilution factor due to gel filtration was 1.5-2. Prior to assaying the hybrid SVs were supplemented with 0.2 µM bafilomycinA1 (Calbiochem).

Measurement of glutamate uptake

Glutamate uptake was performed as previously published (Hell et al., 1990; Maycox et al., 1988; Takamori et al., 2000). The uptake was measured with 2 µCi ^{3}H-glutamic acid (GE Healthcare, Hartmann Analytik GmbH) per data point in the presence of 2 mM ATP, 50 µM choline glutamate, 0 - 30 mM choline chloride in uptake buffer (150 mM choline gluconate, 10 mM MOPS-Tris, pH 7.3, 2 mM $MgSO_4$ and either 50 mM choline gluconate, K-gluconate or Na-gluconate). 90 µl LP2 (15-20 µg total protein/sample), proteoliposomes (6-8 µg VGLUT1/sample), hybrid SVs (~ 15 µg total protein /sample) or PC12-LMFs (~60 µg total protein/sample) were mixed with 10 x uptake buffer and incubated for 15 min at 32 °C. Glutamate uptake in Figures 1, S1, S3C and S4C was performed according to (Winter et al., 2005; Zander et al., 2010). ~10 µg LP2 and 2 µCi ^{3}H-glutamic acid (Hartmann Analytik GmbH and GE Healthcare) were used per data point in 150 mM K-gluconate (KGC) or choline gluconate, 20 mM 1, 4-piperazinediethanesulfonic acid; 4 mM EGTA; 2.9 mM $MgSO_4$ (corresponding to1 mM free Mg^{2+}); and 2 mM ATP, adjusted to pH 7.0 with KOH. Uptake was corrected by subtracting non-specific uptake using 30-60 µM FCCP if not stated otherwise.

Acidification

Acidification measurements were performed according to previous publications (Hell et al., 1990; Maycox et al., 1988) using acridine orange (AO, Molecular Probes) as a pH sensitive dye (Palmgren, 1991). Changes in absorbance at 492 nm (ΔAU) were monitored in an Aminco dual-wavelength spectrophotometer using absorbance at 530 nm as reference, giving a read-out of lumenal pH-changes (Hell et al., 1990; Maycox et al., 1988). Usually, 600 - 650 µl buffer (300 mM glycine, 10 mM MOPS, pH 7.3, and 2 mM $MgSO_4$) were mixed in a 1 ml glass cuvette with 50 - 100 µl of VGLUT/TF_oF_1 liposomes (preloaded with 300 mM glycine, 1-3 mM MOPS-Tris, pH 7.3, and 2 mM $MgSO_4$), hybrid SVs (preloaded with 150 mM choline gluconate, 3 mM MOPS-Tris, pH 7.3, and 2 mM $MgSO_4$) or ~50 µg SV fraction (in 320 mM sucrose, 10 mM MOPS-Tris, pH 7.3, and 2 mM $MgSO_4$) containing 10 µM AO and measured at 32 °C. Substrates were added at the following final concentrations: 1.2 mM ATP, 5 nM valinomycin, 20 mM $(NH_4)_2SO_4$, 10 mM choline glutamate, 30 mM

K-gluconate, Na-gluconate, choline gluconate and 1.5 µM Evans Blue. Representative traces are shown in the figures.

Membrane potential

Measurements of changes in membrane potential were carried out using VGLUT1/TF_oF_1 liposomes and hybrid SVs using Oxonol VI (Molecular Probes), an anionic dye used to detect changes in ΔΨ (Hell et al., 1990; Russell, 1984; Shioi et al., 1989). Absorbance changes at 625 nm (ΔAU) and a reference wavelength at 587 nm were detected using the same Aminco dual wavelength spectrophotometer as for AO measurements. Measurements were performed at 32 °C in 600 - 650 µl buffer (300 mM glycine, 1-3 mM MOPS-Tris, pH 7.3, 2 mM $MgSO_4$) with 100-200 µl of VGLUT1/TF_oF_1 liposomes or hybrid SVs and 15 µM OxonolVI. Applied concentrations: 1.5 mM ATP, 5 nM valinomycin, 5 nM nigericin, 5 mM $(NH_4)_2SO_4$, 50 µM FCCP and 30 mM choline chloride, K-gluconate or choline gluconate. Representative traces are shown in the figures.

SPQ measurements

Chloride flux measurements were performed using 6-Methoxy-*N*-(3-sulfopropyl)quinolinium (SPQ) (Santa Cruz Biotechnology) as a chloride sensitive fluorescent dye, which is collisionally quenched by chloride ions (Biwersi et al., 1994; Verkman, 1990). +/-VGLUT1 liposomes were preloaded with 150 mM KCl/30 mM K-gluconate, pH 7.3 and SPQ (10 mM before dialysis) and fluorescence changes at 443 nm (AU) were monitored using a FluroMax-2® Spectrofluorometer with an excitation wavelength of 344 nm. Measurements were carried out with 150 µl liposomes at 32°C in either 180 mM K-gluconate or 150 mM KCl/30 mM K-gluconate, pH 7.3. The applied concentration of valinomycin was 2 nM. Representative traces are shown in the figures.

SUPPLEMENTAL REFERENCES

Bieniossek, C., Richmond, T.J., and Berger, I. (2008). MultiBac: multigene baculovirus-based eukaryotic protein complex production. Curr. Protoc. Protein Sci., Chapter 5, Unit 5.20.

Degrip, W.J., Vanoostrum, J., and Bovee-Geurts, P.H. (1998). Selective detergent-extraction from mixed detergent/lipid/protein micelles, using cyclodextrin inclusion compounds: a novel generic approach for the preparation of proteoliposomes. Biochem. J. *330*, 667-674.